UNIVERSIDADE DA BEIRA INTERIOR

Engenharia

Effect of the Distance Between Impact Point and Hole Position and Non-Perpendicular Holes on the Impact Strength of Composite Laminates (versão corrigida após defesa de dissertação)

Rafael Alexandre Mota dos Santos

Dissertação para obtenção do Grau de Mestre em

Engenharia Aeronáutica

(ciclo de estudos integrado)

Orientador: Prof. Doutor Paulo Nobre Balbis dos Reis

Co-orientador: Prof. Doutor Pedro Vieira Gamboa

Covilhã, Setembro de 2016

Acknowledgement

The conclusion of this work was only possible thanks to the collaboration and help of various people and institutions. I would like to thank the University of Beira Interior and the Polytechnic Institute of Abrantes and the people that work in these institutions for providing the facilities, materials and equipment necessary for this work.

There are, however, people whose particular contributions were invaluable to finishing this work and to which I owe a lot: I would like to thank my thesis advisor, Professor Paulo Nobre Balbis dos Reis, for his invaluable help and support and the amount of personal time that he dedicated to this work, as well as his insights and teachings which made me a better researcher. No matter the hour of the day, he was always willing to help and never shied away from any necessary criticism to allow me to produce the best work he knew I was capable of.

I would also like to thank my co-advisor, Professor Pedro Vieira Gamboa, for not only having helped me greatly with this work but also for being one of the best teachers that I had the pleasure of having had in the Department of Aerospace Sciences and to which I owe a lot of the tools and knowledge that allowed me to complete this work.

To Professor Abílio Pereira da Silva and Professor Carlos Coelho, I would like to thank for their help and availability, which while it was not required from them, they always happily stepped up to help when necessary.

To my friends and colleagues, in particular those without whom I could not have done this work: Chereches Marius, Elena-Ionela Dinu, Hugo Góis, Hugo Graça, Maria Inês Curto, Pedro Sousa, Sara Coelho, Sara Santos and Mrs. Teresa Gonçalves, I would like to thank for not only their help but their patience as well. Not only did each one of them leave their mark on this work and gave me much needed motivation, they also made it much easier to endure it when things did not work according to planned, whether it was inside or outside of the lab and made even the most unwelcome tasks a fun and pleasant experience. I'm glad I could share this experience with every single one of them.

Finally, I would like to thank my family and parents in particular for their support. Without them this work would not have been possible in the first place.

Abstract

The effect of the distance between impact point and hole position and the angle of the hole with the vertical axis was studied. In order to understand this effect, flexural tests were also performed to evaluate the bending strength of CFRP. In terms of distance of the hole, a maximum reduction of 29.7% on the bending load for a distance of 0 mm was found. This reduction was 22.3% on the impact load. In terms of angle of the hole, a maximum load reduction of 15.6% on the bending strength was found and for the impact load this value was found to be 7% for 20º. The fatigue resistance was also studied. An average reduction of 68.5% on the fatigue resistance of GFRP was obtained for an impact energy of 12 J, in the presence of a hole.

Keywords

Bending; Carbon Fibre; CFRP; Composites; Dynamic Testing; GFRP; Glass Fibre; Impact; Mechanical Behaviour; Non-Destructive Testing; Notch; Open Hole

Resumo

O efeito da distância entre o ponto de impacto e posição de um furo e o ângulo do mesmo com o eixo vertical foi estudado. Para avaliar este efeito, foram também realizados ensaios de flexão. Em termos de distância do furo, uma redução máxima da resistência à flexão de 29,7% foi verificada para uma distância do furo de 0 mm. Esta redução foi de 22,3% no carregamento de impacto. Em termos de ângulo do furo, a redução máxima do carregamento foi de 15,6% para a flexão e em relação ao impacto este valor foi de 7%, para um ângulo de 20º. A resistência à fadiga foi também estudada. Foi verificada uma redução média de 68,5% na resistência à fadiga em compósitos de fibra de vidro para uma energia de impacto de 12 J, na presença de um furo.

Palavras-Chave

Comportamento Mecânico; Compósitos; Ensaio dinâmico; Fibra de Carbono; Fibra de Vidro; Flexão; Furo; impacto

Table of Contents

List of Figures

List of Tables

List of Acronyms

ACEE	Aircraft Energy Efficiency
ASC	Average Stress Criterion
ASTM	American Society for Testing and Materials
CFRP	Carbon fibre Reinforced Polymer
CNT	Carbon Nanotubes
CS	Control Sample
FRP	fibre Reinforced Polymer
GFRP	Glass Fibre Reinforced Polymer
GLARE	Glass Reinforced Fibre Metal Laminate
HM	High Modulus
HR	High Resistance
IBS	Impact Bending Stiffness
NDT	Non-Destructive Testing
PAN	Polyacrylonitrile
PEEK	Polyetheretherketone
PPS	Polyphenylene Sulphide
PSC	Point Stress Criterion
RTM	Resin Transfer Moulding
UHM	Ultra-High Modulus

Introduction

The economic and technological importance of composites, especially in the current age, is undeniable and everything points to an increase in their importance and ubiquity. Composite materials now occupy an established position in various industries, namely the aerospace, the automobile, the sports and civil engineering industries [1–5].

Particularly in the case of the aerospace industry, the push for the use of composite materials started markedly in the 1950s (during the Cold War) and increased in the 1960s and 1970s giving momentum to the research and development of new composites [6]. In recent times, commercial aircraft such as the Boeing 787 were able to shed hundreds of kilograms of mass with the extensive substitution of aluminium alloys for carbon fibre composites in its primary structures [7].

Over the course of the service life and manufacturing of composites low-velocity impacts (which will be defined later in this work) are expected to occur. Foreign body impacts can occur during manufacturing, routine maintenance or use of a composite laminate part or structure. These impacts can take the form of hail, runway debris and collision with other vehicles or animals. These impacts can damage the integrity of the composite while leaving close to no visible damage to the naked eye [8–11]. As such, the study of materials behaviour under short-term loading is of great interest, particularly on such problems as: transportation of hazardous materials, vehicle crashworthiness, safety of nuclear structures subjected to impact by air-borne debris, the vulnerability of military vehicles and structures to impact and protection of spacecraft from meteoroid impacts [11].

Furthermore, it is common for composite structures to require open holes for the passage of electric wires, hydraulic pipes or for assembly or maintenance. The presence of open holes results in a high stress gradient on and around their edges [10,12]. However, the prediction of the strength of notched composite laminates is a difficult matter. This is due to the fact that the laminate configuration strongly affects the nature of the damage [10,12,13]. Green *et al.* [14] conducted research on the effects of open hole dimension on the failure mechanisms of composite laminates subjected to tension and observed over a scaling range of 8 from the baseline specimen a maximum of 64 % reduction in strength. In this work, three distinct failure mechanisms were noted: brittle, where fibre failure occurs through the thickness of the laminate; pull-out, where off-axis plies fail via delamination and matrix cracking; and delamination, where complete gauge section delamination occurs. Additionally, Suemasu *et al.* [15] studied the failure mechanisms of notched composite laminates subjected to compression and observed that the first damage to occur was fibre buckling in the 0º layer and delamination in several interfaces was observed before the final unstable fracture in a laminate with high interlaminar toughness, while sudden failure occurred in a laminate with low interlaminar toughness.

The notched strength of composite materials subjected to tensile or compressive loads has been extensively investigated over the past 30 years and various analytical and

computational models have been developed [12,16–19]. However, in terms of impact loads very few studies can be found in the literature, especially on notched composite laminates. On the other hand, these works simplify the problem by assuming an impact at a fixed distance to the hole and always assume a hole perpendicular to the laminate, which is often not the case in real scenarios. Therefore, the present works aims at filling this gap and providing a better understanding of the failure mechanism and strength of notched composite laminates with the hole at various distances from the point of impact and different angles to the laminate surface.

For this purpose, the present work is divided in several sections, where the first one presents the concepts necessary to understand this work and the state of art about the topic studied. In the second, the materials, equipment and procedure will be explained. In the last part, the results of the study will be presented and discussed, following the conclusions of this work.

1- Composite Materials

Along this section a brief introduction to the history of composites will be made, respective definition and their main characteristics/properties. Finally, the typical applications of those materials, particularly in the aeronautic industry, will be referred.

1.1- Introduction

Materials have such and importance on human life that historical periods of human development have been name after the most influential materials at the time [20].

Contrary to what many people might believe, the concept of a composite material was not invented by human beings. It is found in nature, the most known being wood, which is a composite of cellulose fibres in a matrix of a natural glue called lignin [5]. Composite materials and their uses are therefore, not new. They have been used since antiquity. Early in history it was found that combinations of materials could produce properties superior to those of the separate components. Besides the widespread use of wood and cobb[1] in construction, which were used by ancient Israelites in Egypt, for example, composites have also been used to optimize the performance of conventional weapons, like Mongolian bows and Japanese katana. Mongolians made composite bows by bonding together five pieces of wood to form the core of a bow to witch cattle tendons were bonded on the tension side and strips of cattle horns on the compression side. This assembly was then steamed and bent into an arc shape, wrapped in silk and then cooled slowly to create small, lightweight but powerful bows that could be used on horseback [4,6]. In India, Greece and other countries, husks or straws mixed with clay have been used to build houses for several hundred years [5].

In a broad sense of the word, "composite" means "made of two or more different parts". A composite material consists of an assemblage of two or more different materials of different natures and in different phases, completing and allowing the obtainment of a material with characteristics that are superior to those of the separate components. This definition includes a wide assortment of materials, such as fibre reinforced polymers, wood laminates, ceramic mixtures and even some alloys [6,21,22]. Due to the breadth of the materials encompassed under this definition, this work will focus on fibre reinforced composites. This particular category of composite material is composed of a binder or matrix that surrounds and holds in place the fibres or reinforcements (both will be explored further in this work). Fibre reinforcement is preferred because most materials are much stronger in fibre form than in their bulk form. This is attributed to the sharp reduction in the number of defects in the fibres compared to those in bulk form [20].

Although composites have been used throughout history, only in the 1950s did these materials start capturing the attention of industries with the introduction of polymeric-based

[1] Cobb is a natural building material made from subsoil, water, a fibrous organic material (typically straw) and sometimes lime [87].

composites. The history of modern composites arguably began when a salesman from the Owens-Cornering Fiberglass Company began selling fiberglass to interested parties around the United States and these costumers found that fiberglass suited their needs. Fiberglass was made almost by accident in 1935, when an engineer became curious with a fibre that formed during the process of applying lettering to a glass milk bottle. The initial product made of this fine thread of molten glass was used as insulation (glass wool) but structural products followed. This salesman soon realized that the aerospace industry was a likely customer for this newly discovered material [6,23,24]. Early large-scale commercial applications of composite materials started during World War II (late 1940s and early 1950s) with marine and aircraft applications for the military [5]. Not only were even more aircraft being developed and, therefore, composites more widely used in tooling, but the use of composites for structural and semi-structural parts of the airplanes themselves was being explored and adopted. For instance, in the frantic days of the war, among the last parts of an aircraft to be designed were the ducts. Since all the other systems within the aircraft were already fixed, the ducts were required to go around them. This often resulted in ducts that twisted and turned around the other components, usually in very difficult-to-access locations. Metal ducts just could not be easily made in these convoluted shapes. Composite materials seemed to be the answer. The composites were hand laid-up on internal moulds, which were made in the required shape and allowed difficult forms to be more easily achieved [6].

Since then, composite materials have become common engineering materials and are designed and manufactured for various applications, such as automotive components, sporting goods, aerospace parts, consumer goods, and in the marine and oil industries. Nowadays, composite materials increased their application in such industries as consequence of the importance given by the global market to the lightweight components/products. **Figure 1.1** shows, for example, a comparison of some properties between composites and metals. Among all materials, composite materials have the potential to replace widely used steel and aluminium parts, and many times with better performance. Replacing steel components with composite components can save 60 % to 80 % in component weight, and 20 % to 50 % weight by replacing aluminium parts [5]. **Table 1.1** compares some properties of selected materials, including composite materials.

Processing is the name given to the techniques that allow the transformation of materials from one shape into another. Since composite materials involve two or more materials, these techniques are quite different than the ones used for metals processing. **Figure 1.2** classifies the composites and the most used processing techniques in the composites industry (the processes used to produce the specimens used in this research will be briefly explained later in this work). The mixture of fibres and matrix does not become a composite material until the last phase of fabrication: when the matrix is hardened. After this phase it becomes impossible to alter the materials, as in the same way one would modify the structure of a metal alloy using heat treatments, for example [4].

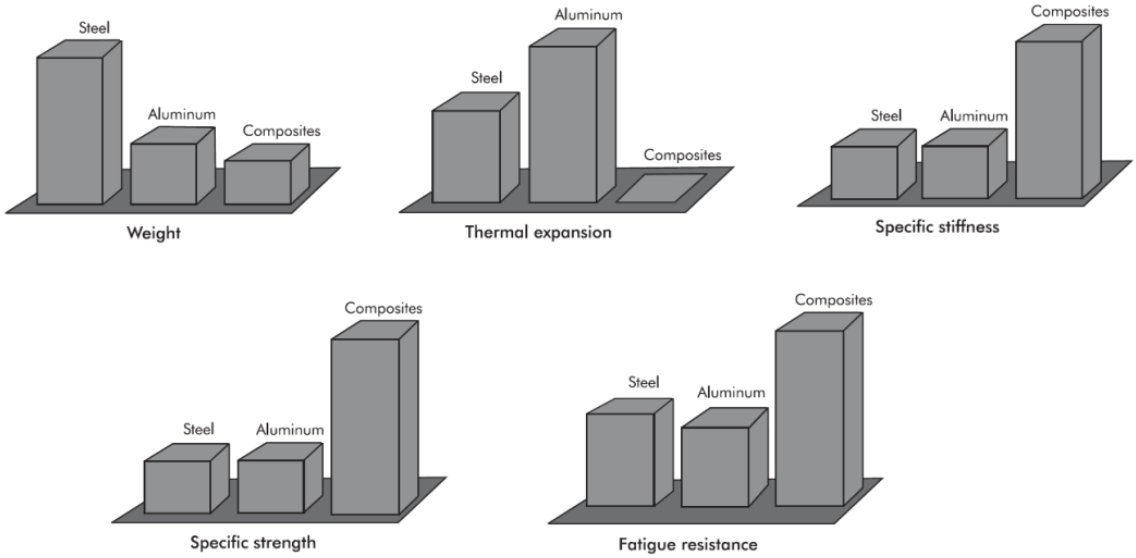

Figure 1.1- Visual property comparison of composites and metals [6].

Table 1.1- Typical properties of some engineering materials [5].

Material	Density (ρ) [g/cm^3]	E [GPa]	σ_{uts} [GPa]	E/ρ	σ_{uts}/ρ	T_{max} [°C]
Metals						
Cast iron, grade 20	7.0	100	0.14	14.3	0.02	230-300
Steel, AISI 1045 hot rolled	7.8	205	0.57	26.3	0.073	500-650
Aluminium 2024-T4	2.7	73	0.45	27.0	0.17	150-250
Aluminium 6061-T6	2.7	69	0.27	25.5	0.10	150-250
Plastics						
Nylon 6/6	1.15	2.9	0.082	2.52	0.071	75-100
Polypropylene	0.9	1.4	0.033	1.55	0.037	50-80
Epoxy	1.25	3.5	0.069	2.8	0.055	80-215
Phenolic	1.35	3.0	0.006	2.22	0.004	70-120
Ceramics						
Alumina	3.8	350	0.17	92.1	0.045	1425-1540
MgO	3.6	205	0.06	56.9	0.017	900-1000
Short fibre composites						
Glass-filled epoxy (35 %)	1.90	25	0.30	8.26	0.16	80-200
Glass-filled polyester (35 %)	2.00	15.7	0.13	7.25	0.065	80-125
Glass-filled nylon (35 %)	1.62	14.5	0.20	8.95	0.12	75-110
Glass-filled nylon (60 %)	1.95	21.8	0.29	11.18	0.149	75-110
Unidirectional composites						
S-glass/epoxy (45 %)	1.81	39.5	0.87	21.8	0.48	80-215
Carbon/epoxy (61 %)	1.59	142	1.73	89.3	1.08	80-215
Kevlar/epoxy (53 %)	1.35	63.9	1.1	47.1	0.81	80-215

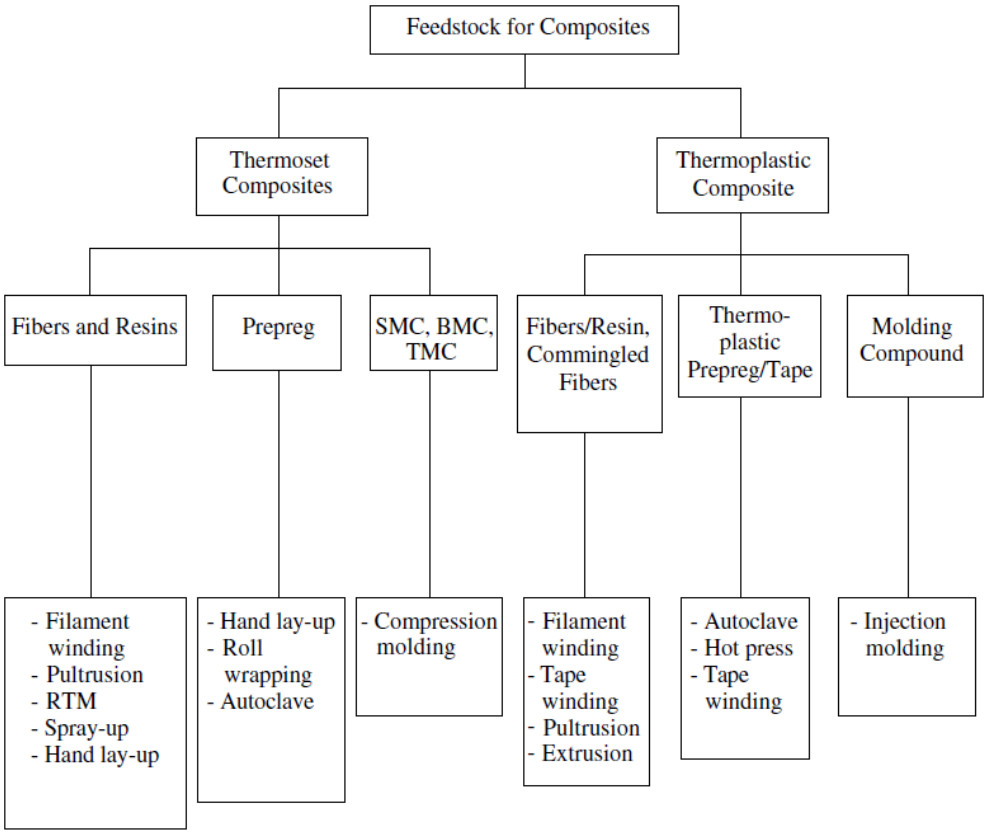

Figure 1.2- Classification of composites processing techniques [5,21].

From all these manufacturing processes, details will be presented only for the techniques used in this work (the hand lay-up process). The simplest and oldest of the fabrication processes for FRP composites, hand lay-up, is a labour-intensive method suited especially for low-volume production of large components such as boat hulls and associated parts. The hand lay-up process may be divided into four basic steps: mould preparation, gel coating, lay-up, and curing. A pigmented gel coat is first sprayed onto the mould for a high-quality surface finish. When the gel coat has become tacky, reinforcing mat and/or woven roving is placed on the mould, and resin is poured, brushed or sprayed on. Manual rolling then removes entrapped air, densifies the composite and thoroughly wets the reinforcement with the resin. Additional layers of mat or woven roving and resin are added for thickness. Curing is initiated by a catalyst or accelerator in the resin system, which hardens the composite without external heat. Hand lay-up offers low-cost tooling, simple processing and a wide range of part size potential. Design changes are made easily. Parts have one finished surface and require trimming [20,25]. **Table 1.2** lists some of the advantages and disadvantages of the hand-layup process.

Prepreg is a pre-impregnated fibre-reinforced material where the resin is partially cured or thickened. The fibres are arranged in a unidirectional tape, a woven fabric, or random chopped fibre sheets. The basic difference between prepreg lay-up and the conventional hand lay-up is that when using prepreg the impregnation of the fibres is made prior to moulding. Prepregs are widely used for making high performance aerospace parts and complex

geometries. Most prepregs are made from epoxy resin systems and reinforcements and usually include glass, carbon, and aramid fibres. In most of the Prepreg systems the resin content is higher than desired in the final part. The removal of this excess resin assists in removing the entrapped air and volatiles that may produce voids in the final part if not removed. This is necessary because for each 1% of voids there is 7% reduction in the intralaminar shear strength and significant reductions in the compressive strength occurring for void content above 2%. Lower resin content also reduces the weight and cost without affecting the strength [20].

The manual lay-up system involves laying plies of pre-cut prepreg into a mould. To begin the lay-up, sufficient material is cut from the roll of prepreg for all of the layers of the part to be made. If material remains on the roll of prepreg after the desired amount is cut off, the roll should be returned to the protective plastic bag and sealed. Then, the bag should be returned to the freezer to maintain the maximum amount of shelf life. An autoclave or vacuum is usually required to assist in consolidating and curing parts laminated with prepregs [6,20]. Some of the advantages and disadvantages of using prepreg are listed in **Table 1.3**.

Table 1.2- Advantages and disadvantages of the hand lay-up process [20].

Advantages	Disadvantages
Large parts with complex geometries can be produced	Only one surface of the moulded part is smooth
Minimal equipment investment	Quality depends on the skill of workers
Minimal tooling cost	Labour intensive
Void content under 1 %	Low production rate
Sandwich construction is possible	High emission of volatiles
Inserts and structural reinforcements can be easily accommodated	Product uniformity is difficult to maintain
Parts requiring excellent finish can be easily manufactured	Long curing times at room temperature
Curing ovens are not necessary	

Table 1.3- Advantages and disadvantages of using prepregs [6,20].

Advantages	Disadvantages
High fibre volume fractions	Slow and labour intensive
Uniform fibre distribution	More expensive curing equipment
Simplified manufacturing	Added cost of making prepreg

1.2- Fibres

Fibres take the form of thousands of filaments that have a diameter between 5 μm and 15 μm, which allow them to be produced using textile techniques and machines. These reinforcements confer the composite their main mechanical characteristics: stiffness, strength,

hardness, density etc. and they are selected in order to improve specific physical properties for a given application: thermal properties, fire resistance, resistance to abrasion and corrosion, electrical properties, etc. and represent a volume fraction of the composite material lying between 0.3 and 0.7 [4,21]. The main function of the fibres are to carry the load (70% to 90% of the load is carried by the fibres); to provide stiffness, strength, thermal stability and other structural properties and to provide electrical conductivity or insulation, depending on the type of fibre used and its application [5]. The ideal characteristics of a fibre reinforcement are high mechanical characteristics, low density, good resin compatibility, ease of production, low cost, etc. [21]. **Table 1.4** compares the properties of common types of fibres.

Table 1.4- Properties comparison of typical fibre reinforcements [4,21,23,24,26].

Fibre	Density (ρ) [g/cm^3]	E [GPa]	σ_{uts} [GPa]	E/ρ	σ_{uts}/ρ	Diameter [µm]
PAN Carbon	1.80	275	3.5	152.78	1.94	6
Pitch Carbon	2.0	344	2.1	172.0	1.05	10
Rayon Carbon	1.60	41	1.0	25.63	0.63	8
HR Carbon	1.75	230	3.5	131.43	2.0	6
HM Carbon	1.81	400	2.8	221.0	1.55	6
UHM Carbon	1.95	600	2.0	307.70	1.03	6
A-Glass	2.44	n/a	n/a	n/a	n/a	15
C-Glass	2.52	n/a	n/a	n/a	n/a	15
D-Glass	2.12	90	2.4	42.45	1.13	15
E-Glass	2.6	15	3.4	5.77	1.31	15
R-Glass	2.5	86	3.2	34.4	1.28	10
S-Glass	2.46	90	4.5	36.59	1.83	15
Aramid	1.44	138	2.8	95.83	1.94	n/a
Boron	2.45	400	6.0	163.57	2.45	150

For this study, carbon and glass fibres were used. The first ones are based on graphite, which has a hexagonal structure of carbon arranged in parallel crystallographic planes. These planes are arranged in such a way that a carbon atom is located in middle of a hexagon of neighbouring planes. The bonds between carbon atoms in neighbouring planes are weak and give the graphite good thermal and electrical conduction properties. In contrast, the bonds between neighbouring atoms in the same plane are strong and give the graphite high mechanical properties in the direction parallel to the crystallographic planes. Theoretical studies of the bonds predicts a Young's modulus of 1200 GPa and a tensile strength of 20 GPa [4,21]. This makes carbon a very suitable material for reinforcement of composites, with great flexibility in its properties. Carbon fibres have very good mechanical properties, particularly given their low density (usually less than 2 g/cm^3). It should also be noted that carbon fibres have an excellent behaviour with temperature in a no oxidising atmosphere. In fact, their mechanical properties are stable up to 1500ºC. This characteristic has led to the development of carbon

fibres/carbon matrix composites with a high temperature resistance, used in rocket nozzles, brake blocks, oven elements, etc. These materials, when covered with an antioxidant layer also find applications in an oxidant atmosphere in space applications [21,23].

Carbon and graphite fibres are produced using PAN-based or pitch-based precursors. The precursor undergoes a series of operations. In the first step, the precursors are oxidized by exposing them to extremely high temperatures. Later, they go through carbonization and graphitization processes. During these processes, precursors go through chemical changes that yield high stiffness-to-weight and strength-to-weight properties. PAN refers to polyacrylonitrile, a polymer fibre of textile origin. Pitch fibre is obtained by spinning purified petroleum or coal tar pitch. PAN-based fibres are most widely used for the fabrication of carbon fibres. Pitch-based fibres tend to be stiffer and more brittle [4].

On the other hand, continuous glass fibres, first conceived and manufactured during 1935 in Newark, Ohio, started a revolution in reinforced composite materials which by 2000 led to a global annual glass fibre consumption of 2.6 million tons. During 1942 glass fibre reinforced composites were first used in structural aerospace parts. In the early 1960s high strength glass fibres, S-Glass, were first used in joint work between Owens Corning Textile Products and the United States Air Force. Later in 1968, S-2 Glass® fibres began evolving into a variety of commercial applications [23,24].

Glass in bulk form is characterized by great brittleness, attributed to a high sensitivity to cracking. In contrast, when made in the form of fibres of small diameter (some tens of micrometres) glass loses this character and then has good mechanical characteristics. Glass fibres are made by starting from a mineral glass, composed of silica, alumina, lime, magnesia, etc. These low cost products, associated with quite simple production processes, give glass fibres an excellent price/performance ratio, which puts them in the first rank of reinforcements actually used in composite materials [21,27]. Glass fibres are produced by feeding the raw glass into a fiberizing element referred to as a "bushing", made of a platinum-rhodium alloy, and pierced in its base by calibrated orifices about 2 mm in diameter. The molten glass is kept in this vessel, heated by the Joule effect, at about 1250°C. At this temperature the viscosity of glass allows a flow under gravity through the orifices in the form of fibres of some tens of millimetres. At the exit of the bushing the glass, in a plastic phase, is simultaneously drawn at high speed and cooled. The cooling conditions and speed of drawing allow either continuous or discontinuous fibres to be obtained, of determined diameters (usually 5 to 15 micrometres) [21,27].

Glass fibres fall into two categories, low-cost general-purpose fibres and premium special-purpose fibres. Over 90% of all glass fibres are general-purpose products. These fibres are known by the designation E-glass and are subject to ASTM specifications. The remaining glass fibres are premium special-purpose products. Many, like E-glass, have letter designations implying special properties. Some have tradenames, but not all are subject to ASTM specifications [26,28]. **Table 1.5** summarizes the different types of glass available which can be converted into usable fibres.

Table 1.5- Different types of glass [21,24,26].

Designation	Characteristic
A	High alkali or soda lime glass (low electrical resistivity)
C	High chemical durability (corrosive environments)
D	High dielectric values (electrical applications)
E	Low electrical conductivity (general use)
M	High stiffness
R, S	High mechanical properties (high performance use)

Glass composites have gained advantages relatively to carbon and aramid composites in certain applications. Cost per weight or volume, certain armament applications, chemical or galvanic corrosion resistance, electrical properties, and availability of many product forms remain as examples of this advantage. Coefficient of thermal expansion and modulus properties compared to carbon composites may be considered as typical disadvantages. When compared to aramid composites, glass has a disadvantage as to tensile properties but an advantage as to ultimate compression, shear properties, and moisture pick-up. Commercial uses for glass products are numerous. These include filtration devices, thermal and electrical insulation, pressure and fluid vessels, and structural products for automotive and recreation vehicles. Many uses are applicable to military and aerospace products as well. A partial listing would include: asbestos replacement, circuitry, optical devices, radomes, helicopter rotor blades, and ballistic applications. Because of the many product forms, structural applications are limitless to fabricate. If there are limitations, compared to other fibres, they may include low thermal and electrical conductivity or perhaps low melting temperatures when compared to carbon fibres [23].

1.3- Matrices

The matrix itself comprises a resin (polyester, epoxide, etc.) and fillers, the goal of which is to improve the characteristics of the resin while reducing the production cost. From a mechanical point of view, the filler-resin system behaves as a homogeneous material [21]. The matrix surrounds the fibres and thus protects those fibres against chemical and environmental attack. For fibres to carry maximum load, the matrix must have a lower modulus and greater elongation than the reinforcement and offer compatibility with the fibres [5,21]. In addition, they must have a low density to keep in the composite's high specific mechanical characteristics. Taking these constraints into account, the resins used are polymers modified by different additives, mould release agents, stabilizers, pigments, etc. Resins are delivered in solution in the form of polymers in suspension in solvents that prevent linking between the pre-polymerized macromolecules. When heated, links develop between the chains of the pre-polymer so as to make a cross-linked polymer with a three-dimensional structure.

Two large families of polymer resins exist: thermosetting and thermoplastic resins [21]. Thermoset materials once cured cannot be remelted or reformed. During curing, they form

three-dimensional molecular chains, called cross-linking. Due to these cross-links, the molecules are not flexible and cannot be remelted and reshaped. The higher the number of cross-links, the more rigid and thermally stable the material will be. In rubbers and other elastomers, the densities of cross-links are much less and therefore they are flexible. Thermosets may soften to some extent at elevated temperatures. This characteristic is sometimes used to create a bend or curve in tubular structures, such as filament-wound tubes. Thermosets are brittle in nature and are generally used with some form of filler and reinforcement. Thermoset resins provide easy processability and better fibre impregnation because the liquid resin is used at room temperature for various processes such as filament winding, pultrusion, and RTM. Thermosets offer greater thermal and dimensional stability, better rigidity, and higher electrical, chemical, and solvent resistance [5].

Thermoplastic materials are, in general, ductile and tougher than thermoset materials and are used for a wide variety of non-structural applications without fillers and reinforcements. Thermoplastics can be melted by heating and solidified by cooling, which render them capable of repeated reshaping and reforming. Thermoplastic molecules do not cross-link and therefore they are flexible and reformable. Thermoplastics can be either amorphous or semi-crystalline. In amorphous thermoplastics, molecules are randomly arranged; whereas in the crystalline region of semi-crystalline plastics, molecules are arranged in an orderly fashion. Their lower stiffness and strength values may require the use of fillers and reinforcements for structural applications. Thermoplastics generally exhibit poor creep resistance, especially at elevated temperatures, as compared to thermosets. They are more susceptible to solvents than thermosets. Thermoplastic resins can be welded together, making repair and joining of parts more simple than for thermosets. Thermoplastic composites do not enjoy as high a level of integration as is currently obtained with thermosetting systems [5]. **Table 1.6** compares the properties of the most commonly used resins in composite materials.

The resins used most widely after the unsaturated polyester resins are the epoxide resins. However, they represent only of the order of 5% of the composites' market on account of their high price (of the order of five times more than polyester resins). Because of their good mechanical characteristics, the epoxide resins, usually used without fillers, are the matrices of high performance composites (aeronautical construction, space, missiles, etc.). Epoxide resins thus lead to a set of high performances. Nevertheless, in order to benefit in actuality from these performances it is necessary to have very long cycles of transformation and long cure times (from several hours to several tens of hours) at relatively high temperatures (50-100°C) [21]. Epoxy is a very versatile resin system, allowing for a broad range of properties and processing capabilities. It exhibits low shrinkage as well as excellent adhesion to a variety of substrate materials.

There are varying grades of epoxies with varying levels of performance to meet different application needs. They can be formulated with other materials or can be mixed with other epoxies to meet a specific performance need.

Table 1.6- Properties comparison of typically used resins [5].

Resin	Density (ρ) [g/cm3]	E [GPa]	σ_{uts} [GPa]
Thermosetting			
Epoxy	1.2 – 1.4	2.5 – 5.0	0.050 – 0.110
Phenolic	1.2 – 1.4	2.7 – 4.1	0.035 – 0.060
Polyester	1.2 – 1.4	1.6 – 4.1	0.035 – 0.095
Thermoplastic			
Nylon	1.1	1.3 – 3.5	0.055 – 0.090
PEEK	1.3 – 1.35	3.5 – 4.4	0.10
PPS	1.3 – 1.4	3.4	0.080
Polyester	1.3 -1.4	2.1 – 3.5	0.055 – 0.060
Polycarbonate	1.2	2.1 – 3.5	0.055 – 0.070
Acetal	1.4	3.5	0.070
Polyethylene	0.9 – 1.0	0.7 – 1.4	0.020 – 0.035
Teflon	2.1 – 2.3	n/a	0.010 – 0.035

By changing the formulation, properties of epoxies can be changed, the cure rate can be modified, the processing temperature requirement can be changed, the cycle time can be changed, the drape and tack can be varied, the toughness can be changed, the temperature resistance can be improved, etc. Epoxies are cured by chemical reaction with amines, anhydrides, phenols, carboxylic acids, and alcohols. The curing (cross-linking) reaction takes place by adding a hardener or curing agent (e.g., diethylenetriamine). During curing, molecules form cross-links with each other. These cross-links grow in a three-dimensional network and finally form a solid epoxy resin [5]. Epoxies are generally brittle, but to meet various application needs, toughened epoxies have been developed that combine the excellent thermal properties of a thermoset with the toughness of a thermoplastic. Toughened epoxies are made by adding thermoplastics to the epoxy resin by various patented processes [5]. **Table 1.7** shows some advantages and disadvantages of using epoxide resins.

Table 1.7- Advantages and disadvantages of epoxide resins [21].

Advantages	Disadvantages
Good mechanical properties (tension, bending, compression, shock, etc.)	Long polymerization time
Good behaviour at high temperatures: up to 150-190°C in continuous use	High cost
Excellent chemical resistance	The need to take precautions at the time of manufacture
Low shrinkage in moulding process and during cure (from 0.5-1 %)	Sensitivity to cracking
Very good wettability of reinforcements	
Excellent adhesion to metallic materials	

1.4- Aerospace Composite Market

There are many reasons for the growth in composite applications, but the primary impetus is that the products fabricated with composites are stronger and lighter. Today it is difficult to find any industry that does not utilize the benefits of composite materials. The largest user of composite materials today is the transportation industry, having consumed 1.3 billion pounds of composites in 2000, as shown in **Figure 1.3**. Composite materials have become the materials of choice for several industries. In the past three to four decades, there have been substantial changes in technology and its requirement. This changing environment created many new needs and opportunities, which are only possible with the advances in new materials and their associated manufacturing technology. In the past decade, several advanced manufacturing technology and material systems have been developed to meet the requirements of the various market segments. Several industries have capitalized on the benefits of composite materials.

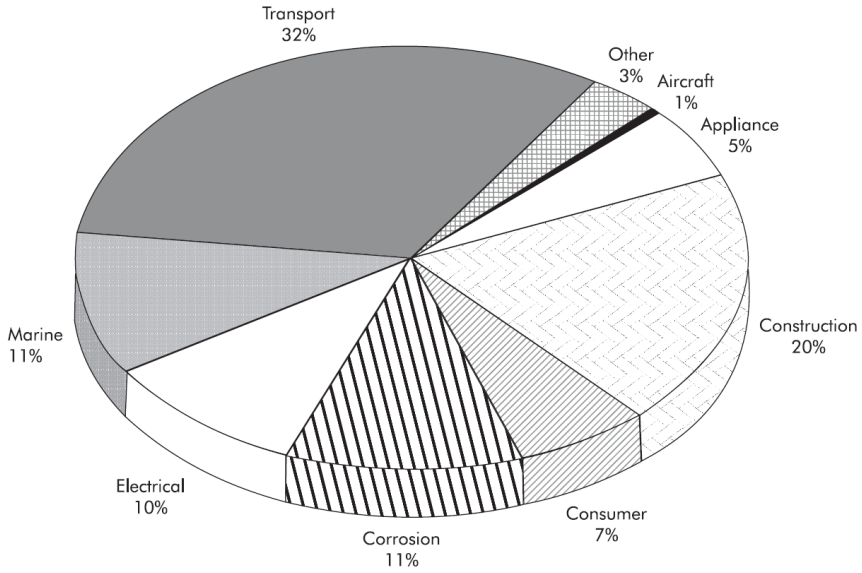

Figure 1.3- U.S. composite shipments [6].

The vast expansion of composite usage can be attributed to the decrease in the cost of fibres, as well as the development of automation techniques and high-volume production methods. For example, the price of carbon fibre decreased from $15000/lb. in 1970 to about $800/lb. in 2000. This decrease in cost was due to the development of low-cost production methods and increased industrial use [5].

The aerospace industry was among the first to realize the benefits of composite materials. Airplanes, rockets, and missiles all fly higher, faster, and farther with the help of composites. Glass, carbon, and Aramid fibre composites have been routinely designed and manufactured for aerospace parts. The aerospace industry primarily uses carbon fibre composites because of their high-performance characteristics. The hand lay-up technique is a common manufacturing method for the fabrication of aerospace parts; RTM and filament

winding are also being used. In 1999, the aerospace industry consumed 23 million pounds of composites. Military aircrafts, such as the F-11, F-14, F-15, and F-16, use composite materials to lower the weight of the structure. The composite components used in the above-mentioned fighter planes are horizontal and vertical stabilizers, wing skins, fin boxes, flaps, and various other structural components as shown in **Table 1.8**. Typical mass reductions achieved for the above components are in the range of 20 % to 35 %. The mass saving in fighter planes increases the payload capacity as well as the missile range. **Figure 1.4** shows the typical composite structures used in commercial aircraft and **Figure 1.5** shows the typical composite structures used in military aircraft. Composite components used in engine applications are shown in **Figure 1.6** [5].

Table 1.8- Composite components in aircraft applications [5,22].

Aircraft	Composite Component	Material	Weight reduction [%]
F-11	Wing fairings	Carbon fibre-epoxy	n/a
Boeing 727	Elevator face sheets	n/a	25
Boeing 737	Spoilers, horizontal stabilizers, wings	n/a	37
F-14	Doors, horizontal stabilizers, fairings, stabilizer skins	Boron fibre-epoxy	19
DC-10	Rudders, vertical stabilizer	n/a	26
L-1011	Ailerons, vertical stabilizer	n/a	25
F-16	Vertical and horizontal stabilizers, fin leading edge, skins on vertical fin box	Carbon fibre-epoxy	23
F-15	Fins, rudders, vertical and horizontal stabilizers, speed brakes, stabilizer skins	Boron fibre-epoxy	25
Boeing 756	Ailerons, rudders, elevators, fairings	n/a	31
Boeing 757	Doors, rudders, elevators, ailerons, spoilers, flaps, fairings	n/a	n/a
Boeing 767	Doors, rudders, elevators, ailerons, spoilers, fairings	n/a	n/a
AV-8B	Doors, rudders, vertical and horizontal stabilizers, ailerons, flaps, fin box, fairings	Carbon fibre-epoxy	25
B-1	Doors, vertical and horizontal stabilizers, flaps, slats, inlets	n/a	n/a
A380	Fuselage and wings skin, doors, tail section	GLARE/Carbon fibre-epoxy	n/a
F-35	Fuselage skins, wing skins, nacelle skins	CNT/Carbon fibre-epoxy	n/a
Boeing 787	Most airframe components	Carbon fibre-epoxy	n/a
A350	Fuselage and vertical stabilizer skins	Carbon fibre-epoxy	n/a

The composite applications on commercial aircrafts began with a few selective secondary structural components, all of which were made of a high-strength carbon fiber

reinforced epoxy. They were designed and produced under the NASA Aircraft Energy Efficiency (ACEE) program and were installed in various airplanes during 1972–1986. By 1987, 350 composite components were placed in service in various commercial aircrafts, and over the next few years, they accumulated millions of flight hours. Periodic inspection and evaluation of these components showed some damages caused by ground handling accidents, foreign object impacts, and lightning strikes. Apart from these damages , there was no degradation of residual strengths due to either fatigue or environmental exposure. A good correlation was found between the on-ground environmental test program and the performance of the composite components after flight exposure [22].

Airbus was the first commercial aircraft manufacturer to make extensive use of composites in their A310 aircraft, which was introduced in 1987. The composite components weighed about 10% of the aircraft's weight and included such components as the lower access panels and top panels of the wing leading edge, outer deflector doors, nose wheel doors, main wheel leg fairing doors, engine cowling panels, elevators and finbox, leading and trailing edges of fins, flap track fairings, flap access doors, rear and forward wing–body fairings, pylon fairings, nose radome, cooling air inlet fairings, tail leading edges, upper surface skin panels above the main wheel bay, glide slope antenna cover, and rudder. The composite vertical stabilizer, which is 8.3 m high by 7.8 m wide at the base, is about 400 kg lighter than the aluminum vertical stabilizer previously used. The Airbus A320, introduced in 1988, was the first commercial aircraft to use an all-composite tail, which includes the tail cone, vertical stabilizer, and horizontl stabilizer. About 25% of its weight is made of composites. Among the major composite components in A380 are the central torsion box (which links the left and right wings under the fuselage), rear-pressure bulkhead (a dome-shaped partition that separates the passenger cabin from the rear part of the plane that is not pressurized), the tail, and the flight control surfaces, such as the flaps, spoilers, and ailerons [22].

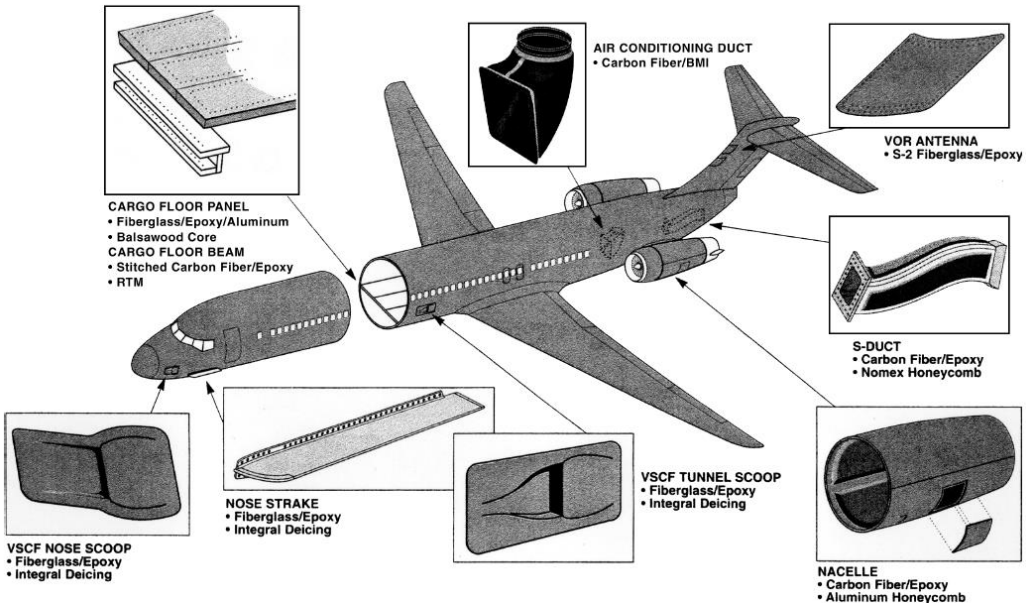

Figure 1.4- Composite structures in commercial aircraft [5].

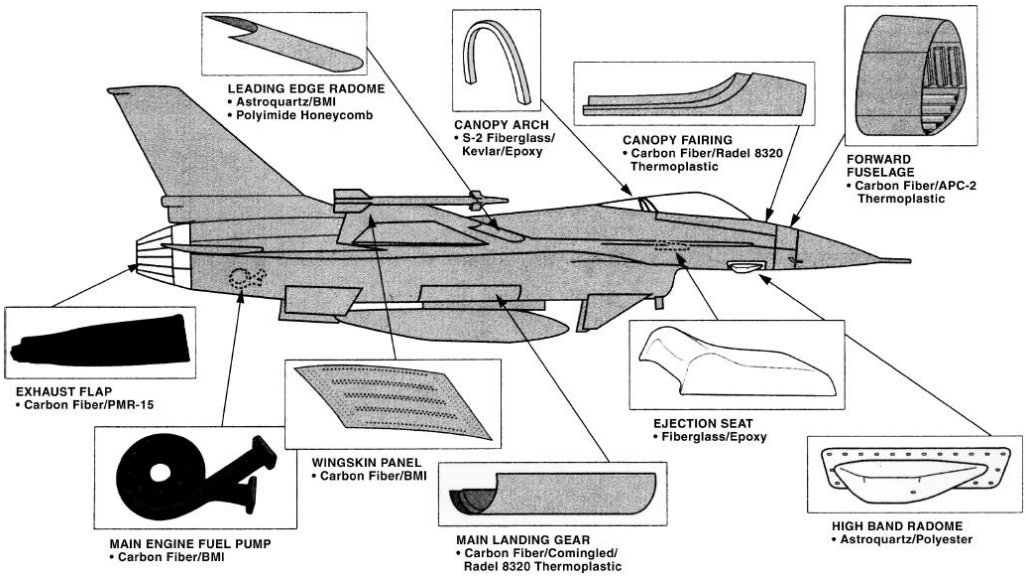

Figure 1.5- Composite structures in military aircraft [5].

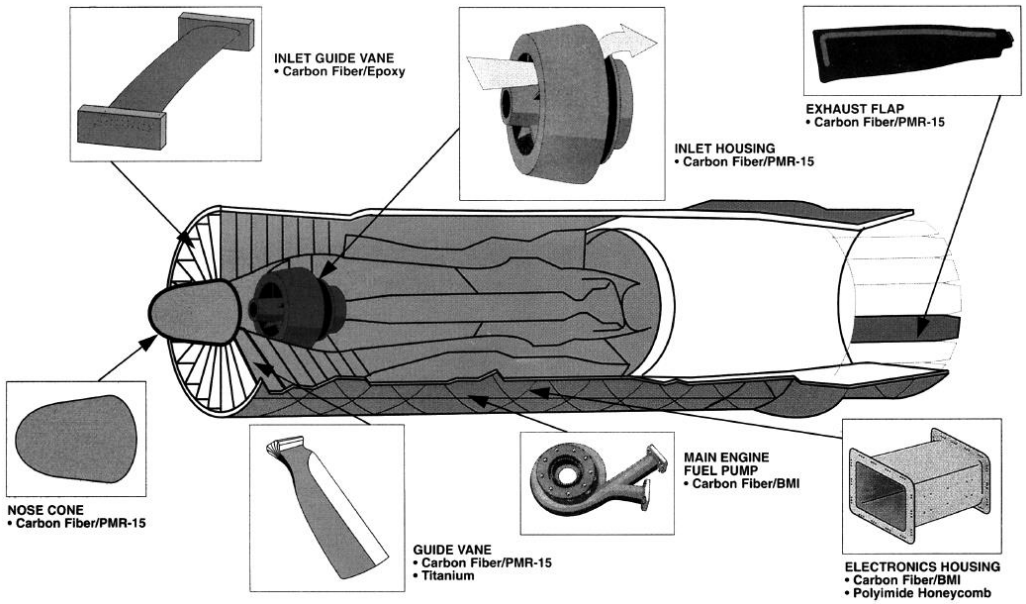

Figure 1.6- Composite components used in engine applications [5].

The main reason for using fiber-reinforced polymers is weight saving, which can lead to significant fuel saving and increase in payload. The key limiting factors in using carbon fibre-reinforced epoxy in aircraft structures are their high cost, relatively low impact damage tolerance (from bird strikes, tool drop, etc.), and susceptibility to lightning damage. When they are used in contact with aluminium or titanium, they can induce galvanic corrosion in the metal components. The protection of the metal components from corrosion can be achieved by coating the contacting surfaces with a corrosion-inhibiting paint, but it is an additional cost [22].

2- Impact in Composite Materials

Along this section the phenomena of impacts in composite materials will be explained. Firstly, the impact will be defined from the point of view of various authors, then a brief explanation about the damage and failure mechanisms of composite laminates subjected to impact will be made, followed by a state of the art review about the research conducted on impact on composite laminates, and in particular on notched laminates. Finally, an introduction to non-destructive damage tests in composite materials will be presented.

2.1- Introduction

Impact may be defined as the relatively sudden application of an impulsive force, to a limited volume of material or part of a structure. The problem is that "relatively" and "limited" can elicit an extraordinarily wide range of interpretations. The effects of impact are widely known and yet, analysing the phenomenon and relating the effects to the forces acting and the materials' properties, in order to predict the outcome of a particular event, can be very difficult. The results of a low velocity impact can be largely elastic, with some energy dissipated as heat, sound, internally in the material, etc. Alternatively, there may be deformation, permanent damage, complete penetration of the body struck or fragmentation of the impacting or impacted body, or even both [3].

As composite materials are used more extensively, a constant source of concern is the effect of foreign objects impacts. Such impacts can reasonably be expected during the life of a structure and can result in internal damage that is often difficult to detect and can cause severe reductions in the strength and stability of the structure [29]. An example of in-service impact occurs during aircraft take-offs and landings, when stones and other small debris from the runway are propelled at high velocities by the tires. During the manufacturing process or during maintenance, tools can be dropped on the structure. In this case, impact velocities are small but the mass of the projectile is larger. Laminated composite structures are more susceptible to impact damage than a similar metallic structure [29].

The lack of plastic deformation in composites means that once a certain stress level is exceeded, permanent damage, resulting in local or structural weakening, occurs. Unlike a metal, which may undergo plastic deformation but can retain its structure, composites stressed above a certain level, though possibly retaining some structural properties, are permanently damaged. A blow with an energy of approximately 1 J or less at about 2 m/s can cause irreversible damage in a realistic composite laminate [3].

Therefore, understanding the mechanisms that lead to failure of composite materials under impact is of great importance to ensure the safety of the structures that use them.

2.2- Classification of Impacts

Generally, impacts are categorized into either low or high velocity and sometimes hyper velocity, but there is not a clear transition between categories and literature is not consensual on their definition [1].

Abrate [29] states that low-velocity impacts occur for impact speeds of less than 100 m/s. However, Cantwell and Morton [30] consider low velocity impacts for velocities up to 10 m/s. On the other hand, Davies and Robinson [1] define low velocity impact when the through-thickness stress wave does not play a critical role in the stress distribution and suggest a simple model to give the transition to a high velocity event. For this, a cylindrical zone under the impactor is considered to suffer a uniform strain as the stress wave propagates through the material, giving the compressive strain (ε_c) as:

$$\varepsilon_c = \frac{\text{impact velocity}}{\text{speed of sound in the material}} \qquad (2.1)$$

For failure strains between 0.5% and 1% this gives a transition to a high velocity impact (where stress waves cannot be ignored) at 10 m/s to 20 m/s for epoxy composites.

According to Hodgkinson [31], low velocity impact is defined as having a projectile impact a specimen with speeds in the range of 1 m/s to 10 m/s. Impacts in the speed range of 100 m/s or more are termed ballistic impacts (high velocity), while those at speeds higher than 1000 m/s are termed hyper velocity impacts. Olsson [32], for example, considers low-velocity impact when the contact time is much longer than the period of the lowest vibration mode (therefore the impact can be termed as quasi-static), and the contact force and plate response are in phase.

Ruiz and Harding [33] distinguish three regimes in terms of impact in composite structures: impact velocities of the order of 300 m/s, where the projectile penetrates the target and all damage is confined to a small area around the point of impact; impact velocities within the range of 50 m/s to 300 m/s, where the stress waves originating from the point of impact transmit the load to the rest of the structure (a dynamic analysis is required); and impacts with velocities lower than 50 m/s, where multiple wave reflections take place at the boundaries and quasi-static equilibrium is reached. Sierakowski [34,35] suggest the classification presented in **Table 2.1**. This author uses a characteristic value, given by $\rho V^2/\sigma_y$, where ρ is the density of the material, V the velocity of the impactor and σ_y the average stress in the material. Sjoblom *et al.* [36] and Shivakumar *et al.* [37] define low velocity impacts as events that can be considered quasi-static and in which the impactor velocity varies from 1 m/s to 10 m/s. For these authors, a high velocity impact is dominated by stress wave propagation through the material, in which the structure has no time to respond, promoting a localized damage.

Swanson [38,39] suggests that if the impact mass is more than ten times the "lumped mass" of the target specimen, then the impact can be considered as a low velocity impact and

it can be considered as a quasi-static event and that through-the-thickness stress waves are a major characteristic of impact of a structure by a foreign body. The "lumped mass" is defined as a function of the target shape and its boundary conditions but it is generally about one half the mass of the entire target.

Table 2.1- Classification of impacts according to Sierakowski [34].

Velocity [m/s]	$\rho V^2/\sigma_y$	Classification
2.5	10^{-5}	Quasi-static
25	10^{-3}	Start of plastic behaviour
250	10^{-1}	Low velocity impact
2500	10^{1}	High plastic deformation
25000	10^{3}	Hyper velocity impact

Finally, Zukas [11] considers that low velocity impacts occur for speeds below 250 m/s. Between 500 m/s and 2000 m/s is considered high velocity, and the structural response becomes secondary for the study of the behaviour of the material in the impacted area. Hyper velocity impact occurs for speeds above 2000 m/s, where local stresses exceed the material strength and the solids being collided can be treated as fluids in the initial instants of the impact. For speeds above 12000 m/s the energy propagation occurs at such a high rate that complete destruction of the materials is likely to occur [34,40]. The classification according to Zukas is presented in **Table 2.2**.

Table 2.2- Classification of impacts and their effects according to Zukas [11,34,40].

Displacement velocity (ε)	Impact velocity [m/s]	Effects	Causes
< 1	< 50	Elastic behaviour with localized plasticity	Mechanic or compressed gasses
1 - 100	50 - 500	Plastic behaviour	Mechanic or compressed gasses
10^2 - 10^4	500 – 1000	Significant viscous response	Solid detonation
10^4 - 10^6	2000 – 3000	Fluid behaviour	Solid detonation
10^6 - 10^7	3000 – 12000	Compressible hydrodynamic impact	Explosive acceleration
10^8	> 12000	Explosive impact	n/a

It should be noted that the range of speeds used by some authors for the definition of low velocity impacts may fall outside the range that can be considered for a viable quasi-static analysis, which presents some practical difficulties [35]. The use of a quasi-static test method for modelling low-velocity impacts is very beneficial to researchers, since much more data can be obtained from a quasi-static test than from an impact test and defects that form during impact, such as matrix cracking can be detected from the energy absorption curves and force-

displacement curves if a quasi-static analysis can accurately approximate a dynamic event [8,36], as shown in **Figure 2.1**.

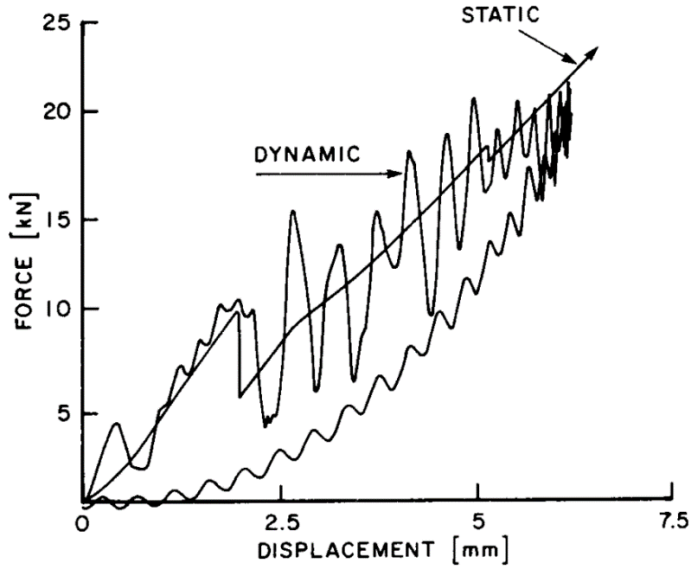

Figure 2.1- Comparison between static and dynamic (impact) response [36].

However, there is no agreement as to whether or not low velocity impacts can be approximated to quasi-static events in the first place. Several authors [8,32,36,37,39,41–43] showed that there is a similarity between a quasi-static indentation and drop-weight impact testing, while others [8,44–46] have shown that there are limitations to the applicability of this correlation. It should be noted that there are numerous variables involved in these testes, such as boundary condition; specimen size, thickness and stacking sequence; impactor size and shape; and type of resin/fibre combination [8].

2.3- Damage on Composite Laminates Due to Impact

Among all the different kinds of damage that composite laminates can suffer, those resulting from impacts are perhaps the most dangerous, since they can be hard to detect. These materials dissipate the impact energy through a combination of various effects, such as [47]:

- matrix cracking;
- fibre breakage;
- delamination;
- fibre-matrix debonding.

Matrix cracking is usually hard to detect and with an increase in stress, the density of the cracks increases and then stabilizes in the laminate. Although matrix cracking does not lead to significant strength reductions, it can contribute to earlier delamination [47].

Since the fibres support most of the stresses suffered by a composite structure, fibre breakage can have a great effect on the mechanical properties of a laminate. This damage is the main mechanism for energy dissipation on impact [47].

Composite laminates are susceptible to delamination damage, mainly due to the lack of reinforcement in the transverse direction and the inherent weakness of their interfaces [48]. Delamination is arguably the most important type of damage in composite laminates subjected to impact, since the increase in delaminations will result in a drastic reduction in the strength and stiffness of the laminate [47].

A laminate subjected to impact will suffer a stress distribution through its thickness that will go from compression on the face that suffers the impact, to tension on the opposite face as a result of the impact-induced flexion [49]. The stacking sequence of the laminate has a major importance on the material strength since it influences its stiffness [50]. Depending on the material stiffness, damage will initiate on the impacted face for stiff laminates, or on the far-side in flexible laminates [8], as show in **Figure 2.2**.

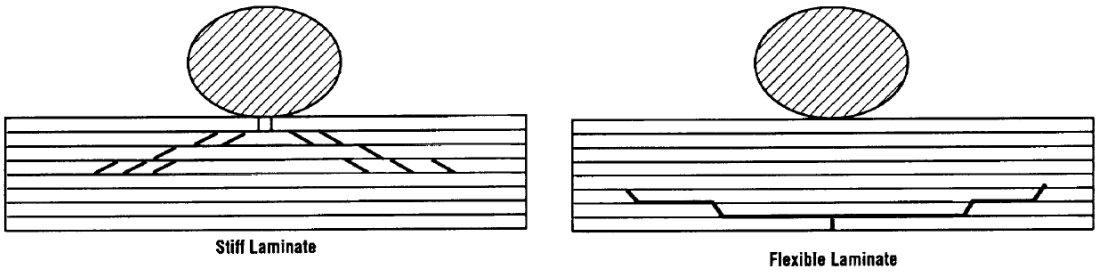

Figure 2.2- Laminate failure modes [8].

Furthermore, delamination by impact will preferentially occur between plies with different orientations, so delamination is less likely to occur between two adjacent plies with the same orientation. Using this rule it is possible to predict the number of delamination that will occur, using a set of equation proposed by Suemasu and Majima [51] to describe the damage initiation and the relation with an external force for different laminates.

2.4- Impact in Notched Laminates

The sensitivity of a composite laminate to a notch was studied by some authors and they showed that it is dependent on a large number of parameters, such as laminate size and thickness, notch size and geometry, width/diameter ratios, ply orientation and thickness, machining quality and material properties [16,52,53]. All of these factors affect the mechanical properties of the laminate by changing the extent of damage growth during loading, and interact with each other to enhance the individual effects [52].

For example, in terms of woven fabric composites with holes, the magnitude and severity of strain concentration is strongly influenced by the tensile loading direction, hole geometry and its dimension relative to the unit cell of the plain woven fabrics [54,55]. On the other hand, for 3D woven carbon/epoxy composites, the notched tensile strength is less than 17 % lower than the un-notched tensile strength and it is not very sensitive to the notch size

[18]. For these laminates, the fractured notched samples showed similar failure modes as the un-notched samples, such as warp tow fracture, debonding and matrix cracking [18].

In another work, four different stacking sequences were studied by Achard *et al.* [56], where the importance of the position of 0º plies in the thickness of the laminate was analysed. Authors demonstrated that the 0º plies placed near or at the outer surface split more easily, so the stress concentration near the hole diminished and the final failure was delayed. Therefore, according to the authors, the 0º plies are protected inside the laminate. On the other hand, the general patterns of damage of 45º and 90º plies adjacent to 0º plies were generally quite similar, with a difference only when the 0º plies split. In this case, the local stress fields were modified. Matrix cracking in a ply always occurred before delamination at adjacent interfaces, similar to those identified in impact.

Green *et al.* [52] investigated the effect of scaling on the tensile strength of notched composites. Hole diameter, ply and laminate thickness, were studied as the independent variables, whilst keeping constant ratios of hole diameter to width and length, over a scaling range of 8 from the baseline size. In general, it was observed that the strength decreased when the specimen size increasing (with a maximum reduction around 64 %), however, the reverse trend of strength increasing with in-plane dimensions was found for specimens with plies blocked together. Three distinct failure mechanisms were observed: fibre failure with and without extensive matrix damage, and complete gauge section delamination.

Additionally, Zitoune *et al.* [57] compared two categories of perforated specimens loaded in tension. The holes of the first category were obtained by drilling and for the second they were obtained by moulding. The tensile strength for moulded hole specimens was higher or equal to 30 % compared to those obtained for drilled hole specimens. It was observed different damage mechanisms between drilled holes and moulded holes specimens, and the strain fields showed that the maximum deformation of a drilled hole is twice as high compared to those of a moulded hole.

The effect of size on the strength of composite laminates with central holes loaded in tension and compression was studied by Erçin *et al.* [16]. Specimens presented different hole sizes but with constant width-to-diameter ratios. The open-hole tensile strength was 66-91% higher than the open hole compression strength, being the difference more pronounced for the specimens with the largest dimensions. The detrimental effect of reversing the load from tension to compression is more pronounced in the notched specimens. Comparing the unnotched tensile and compressive strengths, the strength reduction resulting from applying a compressive load is only 48 %.

Waas and Babcock [58] studied the compressive failure in graphite-epoxy laminates containing a single hole. They observed that damage initiates by a combination of fibre micro-buckling and delamination. The 0º ply micro-buckling originates at the hole edges at 80% of the ultimate compressive strength and propagates into the interior of the specimen.

The in-plane compressive fracture behaviour of carbon fibre-epoxy multidirectional laminates containing a single hole was studied by Soutis and Fleck [59], and they reported up

to 40% reduction in the compressive strength. The dominant failure was fibre micro-buckling in the 0º plies.

The compressive behaviour of the pultruded composite plate specimens with and without holes was investigated by Saha *et al.* [60]. A wide range of hole diameter to width ratios was analysed to determine the compressive strength as a function of hole size. The strain at the hole edge increases with the increasing of hole diameter, and the compressive strength was found to be higher for 6.3 mm than the value observed for 12.7 mm thickness. The post failure analysis suggested that the compressive failure mechanisms consist of delamination, fibre micro-buckling and shearing of continuous strand mats layers.

The compressive failure mechanism of quasi-isotropic composite laminates with an open hole was studied by Suemasu *et al.* [15]. Two types of composite systems were investigated to examine the dependence of failure behaviour on the material properties (such as interlaminar toughness). Independently of the laminate, the first damage was fibre micro-buckling in the 0º layer. Some accumulation of damage, such as further fibre micro-buckling in the 0º layers and interlaminar delaminations in several interfaces, was observed before the final unstable fracture in the laminate with high interlaminar toughness, while sudden failure occurred in the laminate with low interlaminar toughness.

In terms of fatigue, Ferreira *et al.* [61] performed experimental tests on specimens with stress concentration induced by transverse holes, and the results obtained agree with similar studies carried out by Curtis [62], Hyakutake *et al.* [63] and Reis *et al.* [64]. They observed that the stress concentration effect is noted only for lower fatigue lives and for fatigue lives of about 10^6 its influence is very small. The effect of the stress concentration factor was also analysed by Ferreira *et al.* [61], using holes with different diameter, and they obtained a negligible effect for glass fibre/polypropylene composites. Similar tendency was observed by Zhou and Mallick [65], where the fatigue strength of specimens with a hole was lower than that of un-notched specimens, but was insensitive to the hole diameter. However, according to Ferreira *et al.* [61], the fatigue strength is affected by the holes' position. The S-N curve for the off-centre holes was lower around 6%, in stress, than the curve obtained for central holes and this phenomenon can be explained by the considerable increase in the normal tension peak loads that occurs at the narrow bridge on one side of the off-centre hole. Finally, it is reported by the literature that the residual strength after some fatigue cycles increases and is greater than static notched strength [66]. This increase in residual strength is explained by the fact that the damage, which develops at the hole, reduces the local stress concentration [66,67].

While the effect of holes or cut-outs has been studied extensively in terms of tensile and compressive behaviour, there are very few works related with impacts at low velocity [68]. This mode of loading is very dangerous, because it promotes damages very difficult to detect [69,70] while the residual properties of the composite materials are significantly affected [2,71-74]

In this context, Green *et al.* [75] reported the first results of an experimental and numerical study to determine the additional damage arising from the presence of holes. They

are responsible by the matrix cracks that occur in the lower lamina, and these multiple cracks can extend from the region directly below the impact to the edge of the holes. In some circumstances, further cracks can emanate from the far side of the holes.

Studies performed by Luo [76] show that, in composites with open holes, the damage consists basically in delamination associated with matrix cracking, but with absence of fibre breakage. Two parallel matrix cracks appear between the impact point and the hole. One crack initiates at the point of impact and propagates towards the hole whereas the other crack initiates near the hole edge and propagates towards the impact centre. These cracks can be initiated by either tension or shear or a combination of both. On the other hand, when the laminates contain two holes, Roy and Chakraborty [68] found that the delaminations initiate at the interface from the inner free edges of the holes and with time, they meet each other forming a big delamination area. Finally, Amaro *et al.* [10] found that the failure morphology is altered by the presence of holes, confirming a complex damage mechanism (interaction between matrix cracking and delamination).

In terms of impact strength, literature does not report any study about this topic because all works are essentially oriented to characterize, by experimental and numerical procedures, the additional damage arising from the presence of holes and respective damage mechanisms.

2.5- Non-Destructive Testing Techniques for Damage Detection

Since damage induced by low velocity impacts is not easily detected and is often complex in natured due to the range of different types, adequate detection is needed to find and characterize this damage. NDT techniques include several methods that are able to detect the damage shape and size without destruction of the structure or component, which is more economically viable [70,77]. There are several NDT techniques that can be used on composites laminates, as shown in **Table 2.3**.

From all these techniques, the ultrasonic technique was the one used in the present work to evaluate the damages of the studied samples, therefore this technique will be explored further. Ultrasound is a very important tool used as the standard for NDT testing and quality control of materials in most industries. In ultrasonic testing, stress waves must be injected into the material or component to be examined and then the transmitted or reflected beams have to be monitored. Piezoelectric transducers or probes are used to both produce and receive acoustic waves. These are capable of converting electrical pulses into vibrations when in the sending mode, and converting mechanical vibrations (stress waves) into electrical signals for analysis when receiving. It is essential that the stress waves propagate efficiently between the transducers and the component under investigation, i.e., a coupling medium is required between the transducer and the component to ensure satisfactory acoustic transmission. Water as well as various greases and gels have been commonly used as coupling media [70,77].

The pulse-echo method is the most widely used ultrasonic method and involves the detection of echoes produced when an ultrasonic pulse is reflected from a discontinuity or a

defect. This method is very often used for flaw location and thickness measurements. The C-scan technique records echo from the interior of the specimen as a function of the position of each reflecting discontinuity within the probed area.

Table 2.3- NDT techniques [34].

Technique	Characteristic	Advantages	Limitations
Radiography	Differential absorption of radiation	Extensive database; Inspection report	Expensive; Deepness of the defect is hard to identify; Requires radiation protection
Computational topography	X-ray technology with digital processing	Defect location is identified; Image visualization controlled by computer	Very expensive; hard to use with low thickness materials
Ultrasounds	Acoustic impedance changes caused by defects	Can be used in thick materials; Can be automated	Deepness of the defect is hard to identify
Acoustic emission	Defects that generate stress waves	Remote and continuous monitoring	Requires the application of stress
Ultrasonic acoustics	Ultrasonic impulses to generate stress waves	Automated; Graphical image	Superficial contact, surface geometry is critical
Thermography	Temperature mapping	Fast; Remote detection; Quantitative	Low resolution for thick samples
Optic holography	3D imaging	No special preparation of the material	Requires sturdy base to avoid vibrations
Foucault currents	Electric changes caused by defects	Easily automated; Moderate costs	Limited to electrical applications and some materials

A C-scan image is constructed by moving the ultrasound beam over the surface of the structure. The C-scan image then shows a plan view of the recorded data, revealing the size, orientation and location of defects. Flaw depth is not normally recorded, though a relatively accurate estimate can be made by restricting the range of depths (gates) within the test-piece that are covered in a given scan. In the literature there are several applications of the ultrasonic C-scan technique for the inspection of composite materials, which are used in advanced structures where the cost of such an inspection is justified, namely in the detection and characterisation of impact damage in carbon/epoxy composite plates, characterisation of the distribution, size and shape of voids in composite materials, and analysis of some special features of the fibre/matrix interface [70]. **Figure 2.3** shows a schematic representation and the equipment used for the C-scan technique.

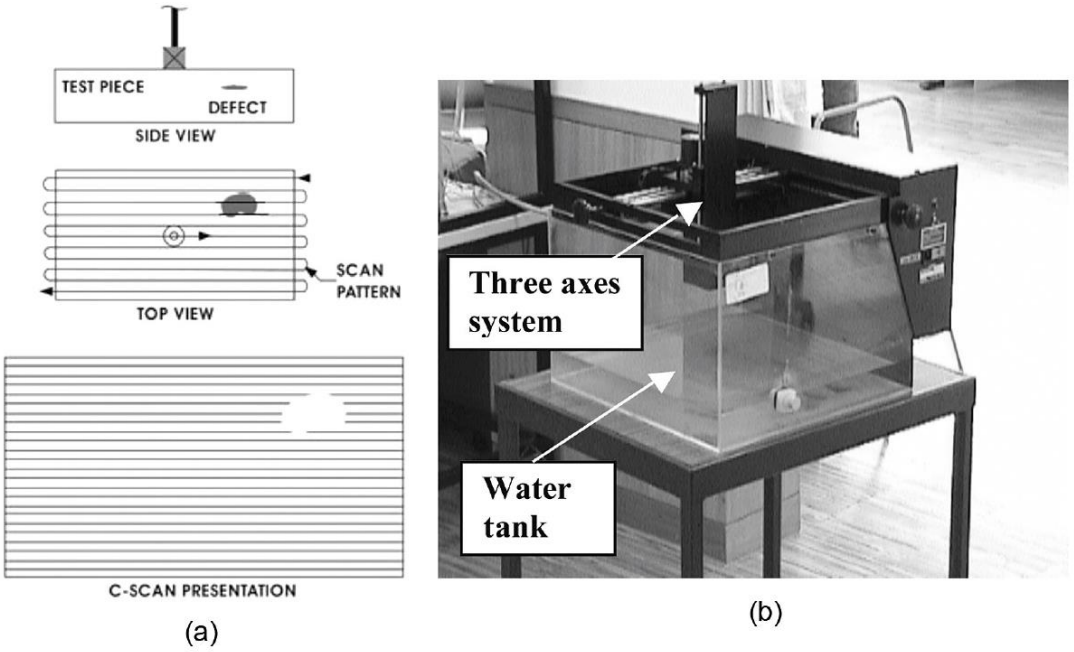

Figure 2.3- C-scan system: (a) Schematic representation; (b) C-scan equipment [70].

3- Materials, Equipment and Procedure

The manufacture process of the specimens used in all experimental tests, as well as the materials and equipment used will be described in this section. Finally, the experimental procedure will be presented in detail.

3.1- Sample Manufacture

Along this study two different laminates were used, according to the objective of the present thesis.

In order to study the effect of non-perpendicular holes and the distance of the hole from the load application on the mechanical properties, composite laminates were prepared in the laboratory. CFRP were made from carbon Prepreg, TEXIPREG® HS 160 REM (provided by SEAL, Legnano, Italy). The CFRP laminates were prepared with sixteen layers, and a stacking sequence of $[0_4,90_4]_s$, using the autoclave/vacuum-bag moulding process in agreement with the manufacturer recommendations (**Figure 3.1**). The processing setup consisted of several steps: making the hermetic bag and applying a 0.05 MPa vacuum; heating up to 125º C at a 3–5º C/min rate; applying a pressure of 5 bar when a temperature of 120-125º C is reached; maintaining pressure and temperature for about 150 min; cooling down to room temperature maintaining pressure and finally getting the part out from the mould. The plates were manufactured in a useful size of 300x300x2.5 mm^3. The quality control was performed by C-Scan, to evaluate the eventual presence of defects resulting from manufacturing process.

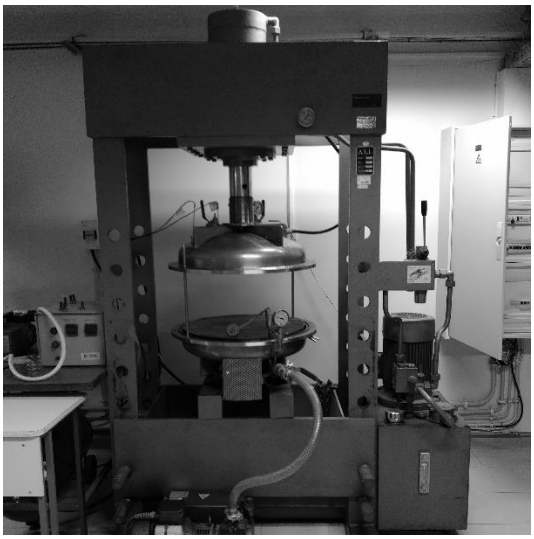

Figure 3.1- Autoclave system.

Finally, for the multi-impact study, GFRP laminates were manufactured. Eight layers of woven bi-directional (0º and 90º) glass fibre, 1195P (195 g/m^2), were prepared by hand lay-up to produce plates with an overall dimension of 330x330x3 mm^3. Biresin® CR122 epoxy resin and a Biresin® CH122-3 hardener, supplied by Sika, was used. The plates were then placed inside a

vacuum bag and a press was used to apply a load of 2.5 kN (**Figure 3.2**) for 12 hours in order to maintain a constant fibre volume fraction and uniform laminate thickness. During the first 4 hours the bag remained attached to a vacuum pump to eliminate any air bubbles existing in the composite. The post-cure was followed according to the manufacturer's datasheet in an oven at 60ºC for 8 hours.

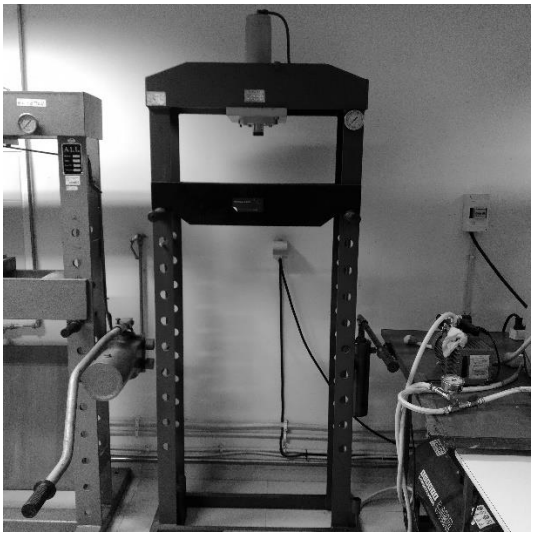

Figure 3.2- Press used for the manufacture of the laminates.

3.2- Samples

The samples were obtained from the laminates described above. The geometry was obtained using a diamond saw (**Figure 3.3**) having, however, special care with the speed. In order to avoid heating up the composite, and consequently cause possible changes in its mechanical properties, water was used to cool down the material and saw.

Figure 3.3- Cutting machine.

Figure 3.4 shows the geometry of the CFRP specimens used in the flexural and impact tests, respectively. These specimens were obtained from the thin plates and the dimensions are, respectively, 100×20×2.5 mm^3 and 100×100×2.5 mm^3. Two parameters were analysed: the distance of the hole from the pin load contact region (0, 5, 10 and 20 mm) and the angle of the hole with the vertical axis (0º, 10º and 20º). For the first parameter (distance) the holes considerate are perpendicular (0º) to the thickness, while for the second parameter (angle) the holes are at 10 mm from the load contact point. All holes have 4 mm of diameter and they were obtained with a special drill for this effect. After drilled, the specimens were evaluated again by C-Scan to verify if any defect was introduced.

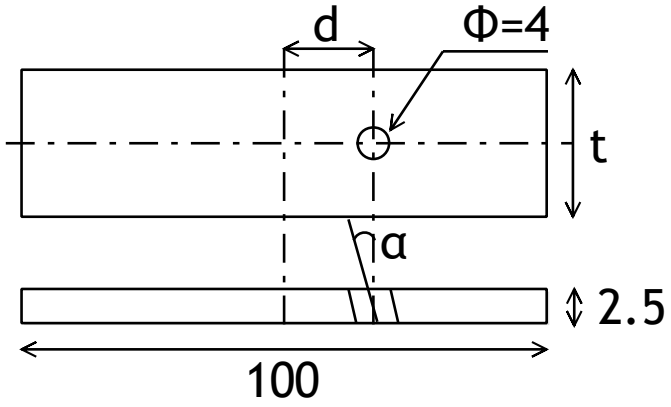

Figure 3.4- Geometry of the CFRP samples (not to scale), dimensions in mm (t=20 mm for flexural tests, t=100 mm for impact tests; d=0, 5, 10 and 20 mm; α=0º, 10º and 20º).

Figure 3.5 shows the geometry of the GFRP specimens used in the multi-impact tests. These specimens were obtained from the thin plates described previously, and the dimensions are 100×100×3 mm^3.

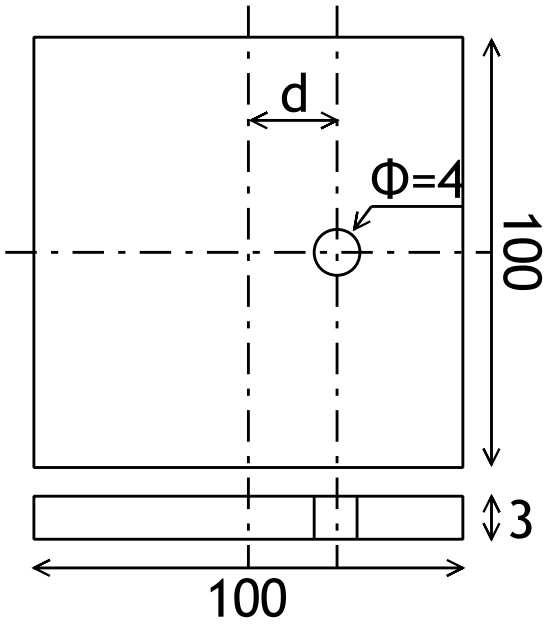

Figure 3.5- Geometry of the GFRP samples (not to scale), dimensions in mm (d=0, 5, 10 and 20 mm).

The distance of the hole to the impact load contact region is 0, 5, 10 and 20 mm and the angle of the hole with the vertical axis is 0º. All holes have 4 mm of diameter and they were obtained with a special drill for this effect. After drilled, the specimens were evaluated to verify if any defect was introduced.

3.3- Equipment

The three-point bending tests were performed using a Shimadzu AGS-X 10 universal testing machine, as seen in **Figure 3.6**, equipped with a 10 kN load cell and TRAPEZIUM software to collect/analyse the results.

Figure 3.6- Flexural testing machine (Shimadzu AGS-X 10).

The low-velocity impact tests were performed using a drop weight-testing machine, IMATEK IM10 as shown in **Figure 3.7**.

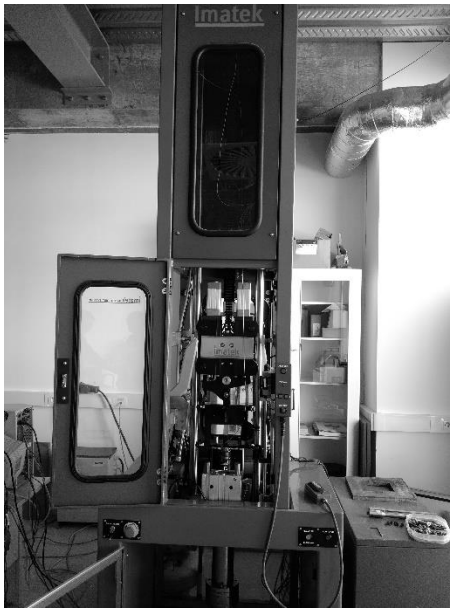

Figure 3.7- Impact testing machine (IMATEK IM10).

The impact energy is completely provided by gravity and controlled by adjusting the high from which the mass is dropped, up to a maximum of 2.5 meters. An optical sensor measures the velocity of the drop weight and the force is measure by a load cell. The double-integration of the load-time curve provides the variation of the deflexion *versus* the load [34]:

$$F(t)=m\frac{d^2x}{dt^2} \qquad (3.1)$$

where $F(t)$ is the force measured by the load cell, m the mass of the drop weight and d^2x/dt^2 is the acceleration of the mass. From equation 3.1 it is possible to calculate the velocity through:

$$V(t)=-\frac{1}{m}\int F(t)\,dt+C_0 \qquad (3.2)$$

where $V(t)$ is the velocity of the weight, C_0 an integration constant which is equal to V_0, the initial velocity, i.e., the boundary conditions for t=0 s. From equation 3.2 we can obtain the displacement as:

$$X(t)=\left(-\frac{1}{m}\int\int F(t)dtdt\right)+V_0\,t \qquad (3.3)$$

where $X(t)$ is the displacement of the load cell [34].

3.4- Experimental Procedure

The three-point bending tests were performed using the specimens and the equipment described previously at a displacement rate of 3 mm/min and tested with a span of 50 mm. All tests were carried out at room temperature and five specimens were tested for each condition according with the ASTM D7264/D7264M–15 standards. The results will be presented in terms of average maximum load.

Finally, the low velocity impact tests were performed, one more time, using the specimens and the equipment described previously. An impactor with a diameter of 10 mm and mass of 2.827 kg was used. The tests were performed on square section samples of 75x75 mm^2 and the impactor stroke at the centre of the samples obtained by centrally clamping the 100x100 mm^2 GFRP specimens and supporting the CFRP specimens. The impact energy used for the tests on the CFRP samples was 3 J and the energy used for the GFRP samples was 12 J. The first energy was previously selected in order to enable the measuring of the damage area using C-scan technique, but without promoting perforation of the specimens, while the second energy level was selected so that the number of impacts to failure was achieved in a reasonable amount

of impacts. For each condition, three specimens were tested at room temperature according to EN ISO 6603-2 standards. The CFRP specimens were subjected to a single impact, whereas the GFRP specimens were subjected to multi-impacts with 12 J of energy until full perforation occurred. Full perforation is defined when the impactor completely moves through the samples.

4- Results and Discussion

This chapter presents all results obtained from the experimental tests performed and respective discussion supported by the open literature. Three sections can be found, where, in the first one, the effect of the angle with the vertical axis will be analysed in terms of flexural and impact strength. In the same context, section two evaluated the effect of the distance between hole and load. During these analyses, and in both cases, the mechanical properties will be discussed in terms of interaction between delamination/holes. For this purpose, CFRP laminates with specific lay-up were used (as discussed previously). Finally, section three presents the results where the multi-impact strength will be evaluated in GRRP laminates with holes at different distances from the impact point.

4.1- Effect of the Hole Angle on Single Impact Strength

A static analysis was carried out in order to evaluate the effects of the angle of the open hole with the vertical axis (α) on the flexural strength of CFRP specimens. **Figure 4.1** shows representative curves of the bending load *versus* flexural displacement for the angles studied (0º, 10º and 20º with the hole at 10 mm from the pin load contact region).

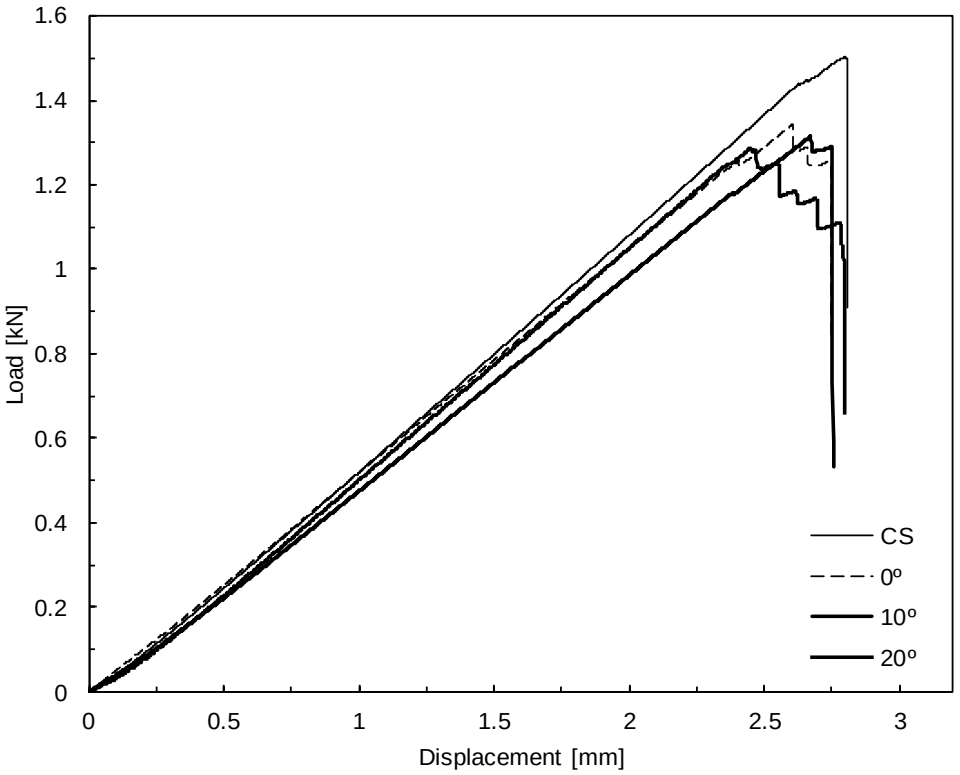

Figure 4.1- Load-displacement curves for the studied angles of the flexural tests.

A nearly brittle behaviour can be observed for all curves obtained with different angles, with a linear region up to the maximum load and a significant drop of the load after peak load

was reached. According with the literature [49,64,72,78], the mechanism of damage is the fracture of the fibres, in compression, with delaminations around the broken fibres. The curves present a zigzag aspect, which results from fibre breakage [64]. The posterior load drop is a consequence of the propagation of delaminations initiated at the regions with broken fibres [64]. All these damage mechanisms can be confirmed by the pictures shown in **Figure 4.2**.

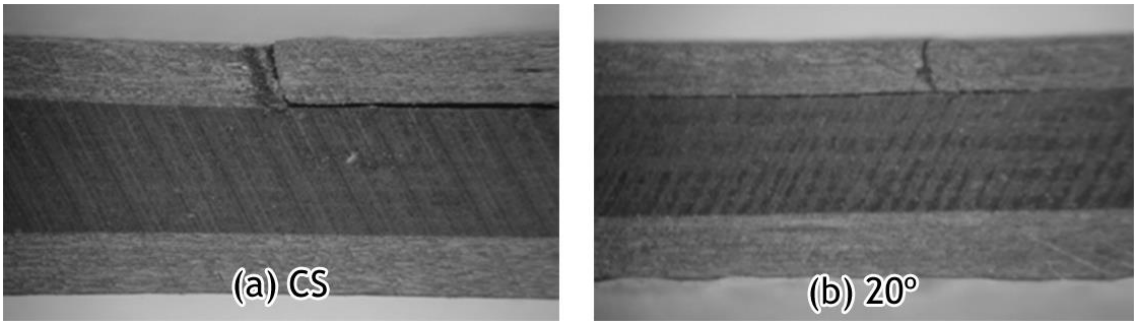

Figure 4.2- Microscopic photography of the damaged area for the studied angles.

Additionally to the stress concentration promoted by the holes, studies developed by Reis *et al.* [78] showed that the high compressive stress concentration in the pin load contact region associated with the low compressive strength of the fibres promotes compressive breakage of the longitudinal fibres in this region.

Figure 4.3 presents the results obtained in the three-point static tests, in terms of maximum load, where the symbols represent the average values and the bands represent, respectively, the maximum and minimum values obtained from the five tests. For laminates without holes (control samples) an average maximum load of 1535 N was found, and this value tends to decrease with the angle of the hole. For example, when the angle is 0º the average maximum load decreases around 12.1%, comparatively to the control samples, but, when the angle is 10º, the maximum load decreases around 12.7%, and for 20º this value is 15.6%. From these results, additionally to the stress concentration promoted by the indentation contact, it is evident the effect of the stress concentration promoted by the hole's presence. Since the difference between the 0º angle and the 10º is negligible, the angle of 10º was not used for the impact study.

In terms of impact tests, **Figure 4.4** shows the force-time and energy-time curves for the first impact. They represent the typical behaviour occurred for all laminates and agree with the bibliography [3,32,36,43,68,72,79–83]. These curves contain oscillations that, according with literature [79], are consequence of the vibrations promoted by the samples. These vibrations depend on the material's stiffness and mass, and according to Belingardi and Vadori [81] are caused by the variation of the kinematic quantities.

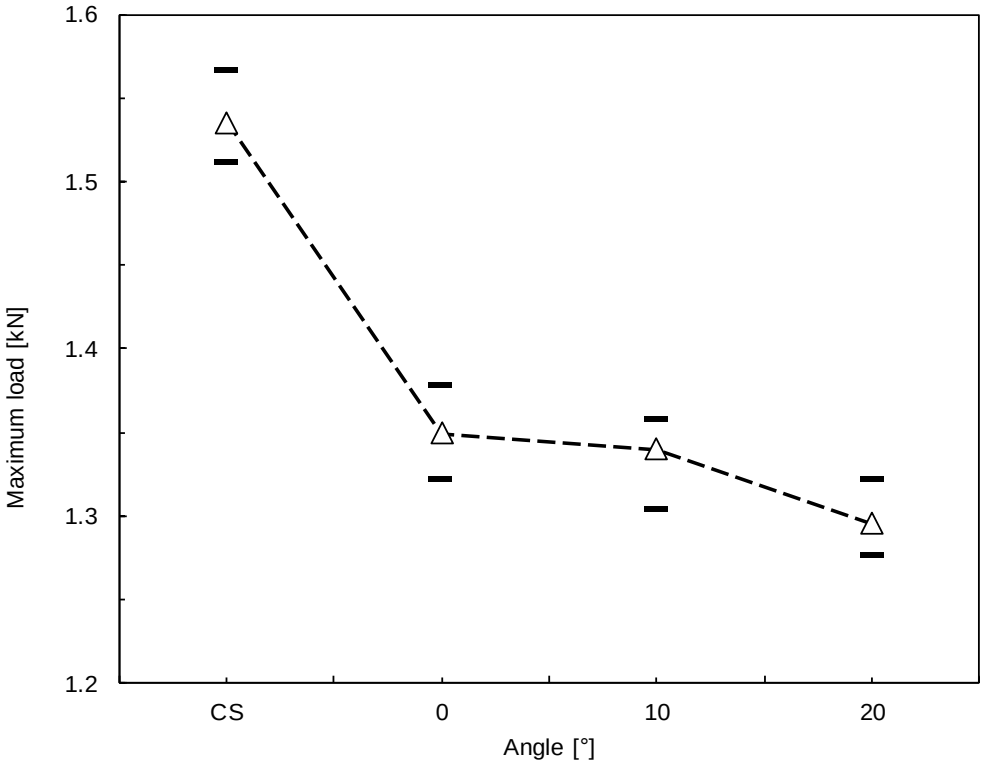

Figure 4.3- Maximum load versus angle of the hole with the vertical axis for the flexural tests.

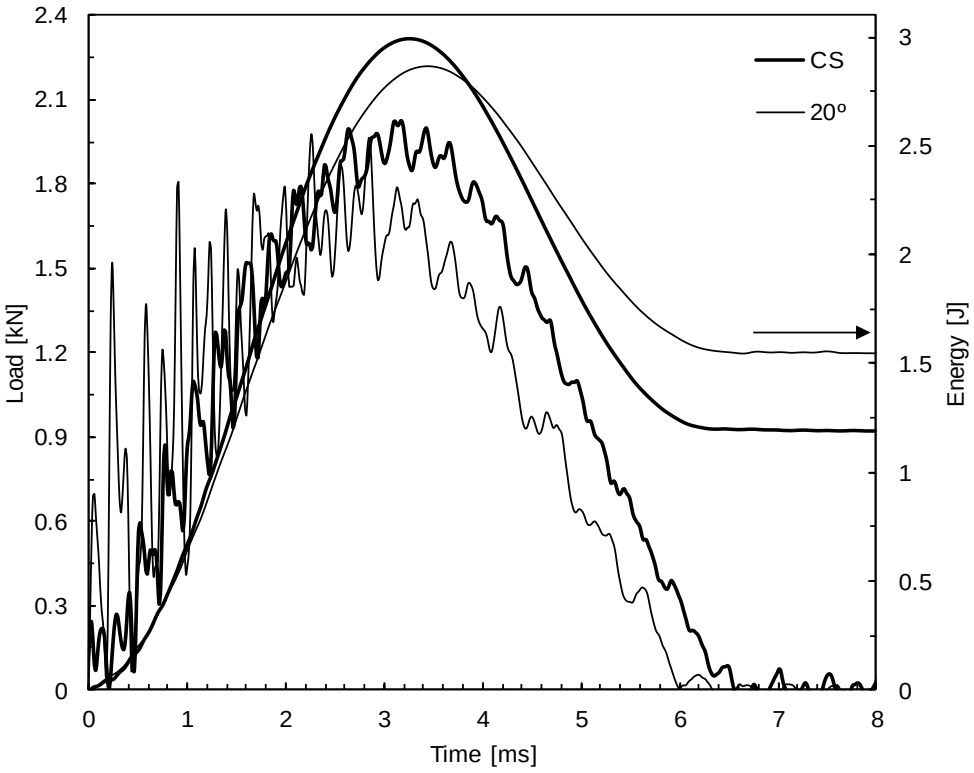

Figure 4.4- Load-time and energy-time curves for the CS and 20º hole for the CFRP samples subjected to impact.

In detail, it is possible to observe that the force increases up to a maximum value, P_{max}, followed by a drop after peak load is reached. The impact energy was not high enough to cause full penetration, because the impactor strikes the specimens and rebounds. In this context non-perforating impact occurred for all laminates. On the other hand, in terms of the curves that represent the evolution of the energy with time, the beginning of the plateau coincides with the loss of contact between the striker and the specimen and, consequently, this energy coincides with that absorbed by the specimen. Therefore, the elastic energy is calculated as the difference between the absorbed energy and the energy at peak load.

Figure 4.5 shows the results obtained for the single impact in terms of maximum load and maximum displacement for the studied angles of the hole. For each angle three tests were performed. For the CS an average maximum load of 2014 N was obtained. This value is 2.3% lower for the hole with a 0º angle and 7% lower for the 20º hole. In terms of maximum displacement, the average value obtained for the control samples is about 3.04 mm and this value increase 1.4% and 4.4% for laminates containing holes with 0° and 20° angle, respectively. The trend described for the maximum load and maximum displacement can be justified by the damage mechanisms associated with the stress concentration at the tip of the hole [14].

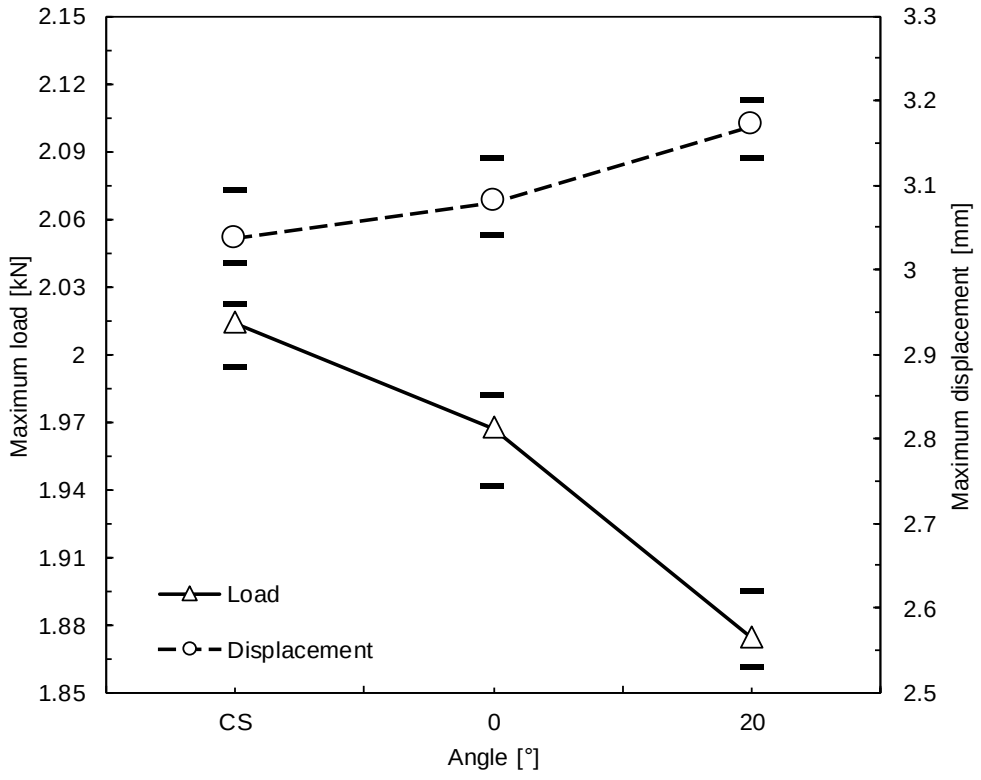

Figure 4.5- Maximum load and maximum displacement versus angle of the hole with the vertical axis for the impact tests.

Figure 4.6 shows the C-Scan obtained for the different laminates. Delaminations present the typical two lobed shape, where the major delamination occurs at the lower interface (between the 90º and 0º layer groups) and is oriented with the adjacent lower fibres' direction, i.e., the 0º layers (in all images the 0º layers are displayed vertically). According with the literature, an extensive crack aligned with the fibres direction of this lowest ply occurs as well as some matrix cracking induced by shearing in the adjacent group of layers (90º). This damage pattern demonstrates an interaction phenomenon between matrix cracking and delamination and reveals a complex damage mechanism. For composites with holes, the failure starts at the location of the highest stress concentration, and grows perpendicular to the loading direction [15]. Finally, it is evident the bigger damaged area of the 20º hole compared to the 0º hole, which explains the decrease in load and increase in displacement.

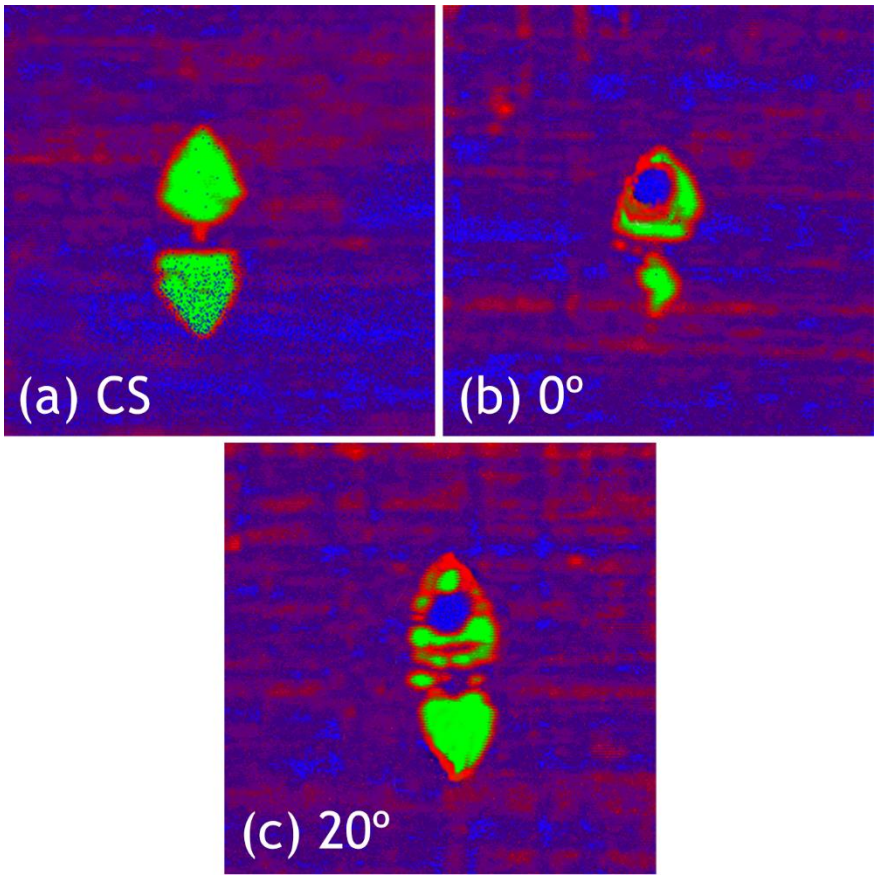

Figure 4.6- C-scan imaging of the CFRP samples subjected to impact.

The impact bending stiffness has been known as an important property in assessing the damage resistance of a composite. Using the load-displacement, the slope of the linear regression of the ascending section of the load-displacement curve, up to the maximum load and displacement, is the impact bending stiffness [84]. **Figure 4.7** presents the IBS and elastic recuperation.

From the figure, it is possible to observe that both variables decrease with an increasing of the angle. For the control samples, for example, the average value of the IBS is

about 635 N/mm and this decreases about 2.6% and 7.9% for 0º and 20º, respectively. This trend agrees with **Figure 4.6**, where the damage increases with the angle of the hole. On the other hand, the elastic recuperation for the control samples was 60%, and this value decreased by 0.8% for the 0º hole and 4.7% for the 20º hole. This decrease in elastic recuperation is necessarily accompanied by an increase in absorbed energy as damage, which agrees with the previous results.

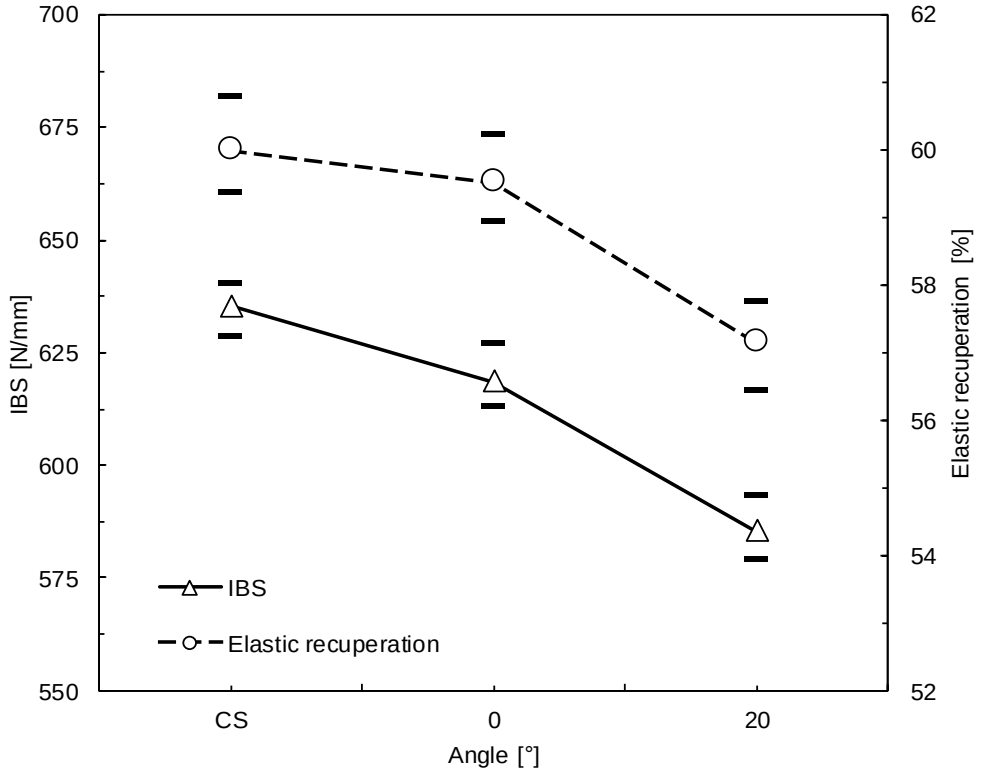

Figure 4.7- IBS and elastic recuperation versus angle of the hole with the vertical axis for the impact tests.

4.2- Effect of the Distance Between the Impact point and Hole Position on Single Impact Strength

Figure 4.8 shows representative curves of the bending load *versus* displacement for the distances considered (0, 5, 10 and 20 mm from the pin load contact region with the hole at 0º with the vertical axis). These curves present a similar behaviour as described previously, where, for all distances, a linear region up to the maximum load and a significant drop of the load after peak load can be found. Consequently, similar damage mechanisms are expected as shown in **Figure 4.9**.

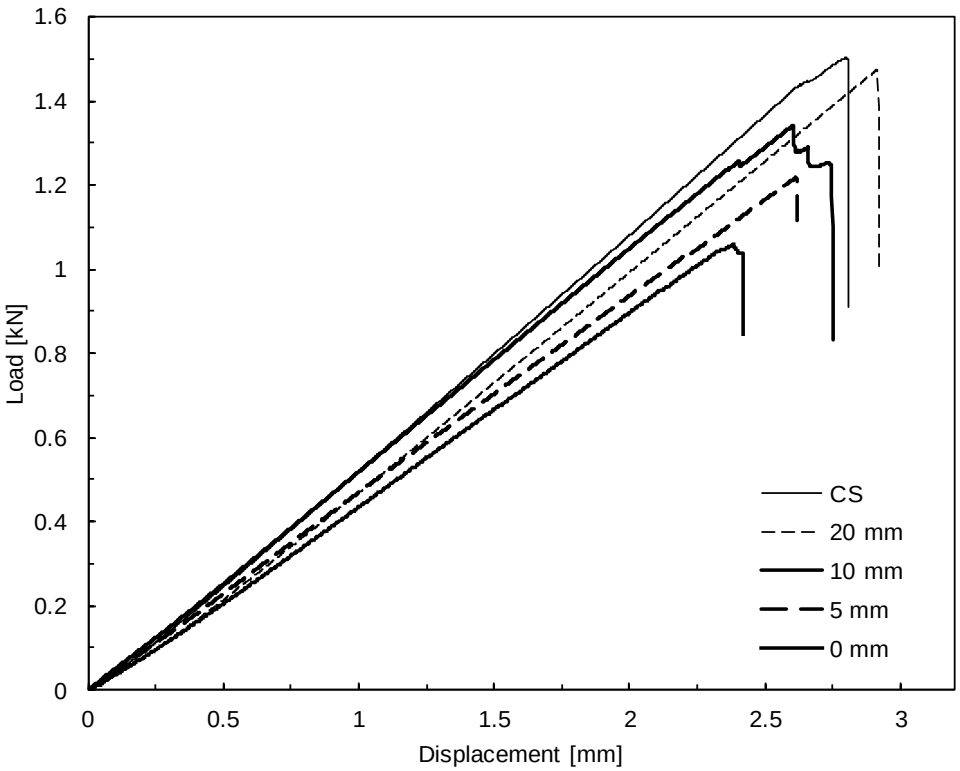

Figure 4.8- Load-displacement curves the studied distances for the flexural tests.

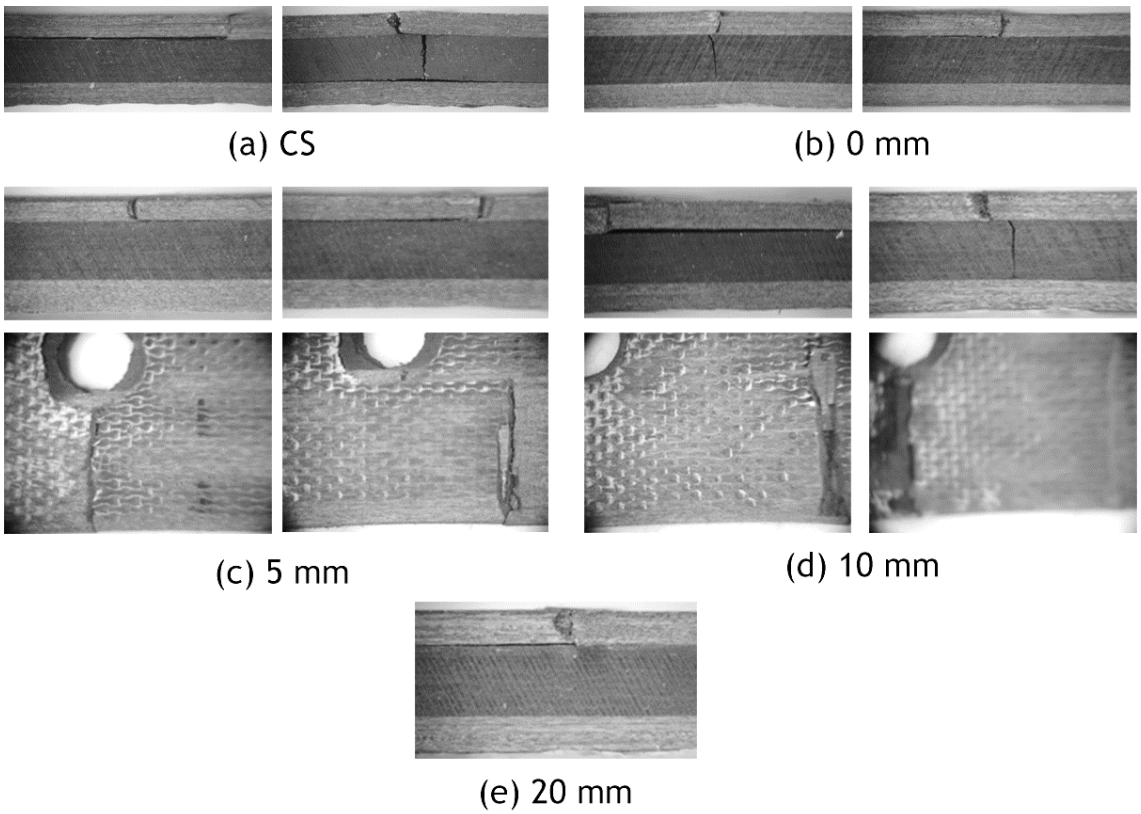

Figure 4.9- Microscopic photography of the damaged area for the studied distances of the flexural tests.

Figure 4.10 presents the results for the effect of the distance obtained with the flexural tests in terms of maximum load. For the CS an average maximum load of 1535 N was obtained. This value decreased by 2.2% for 20 mm, 10.2% for 10 mm, 20% for 5 mm and 29.7% for 0 mm. A significant effect of the distance can be found, but for distances higher than 20 mm this effect tends to dissipate. According to Whitney and Nuismer [85], the failure occurs when the average stress over some distance (a_0) ahead of the notch is equal to the unnotched laminate strength.

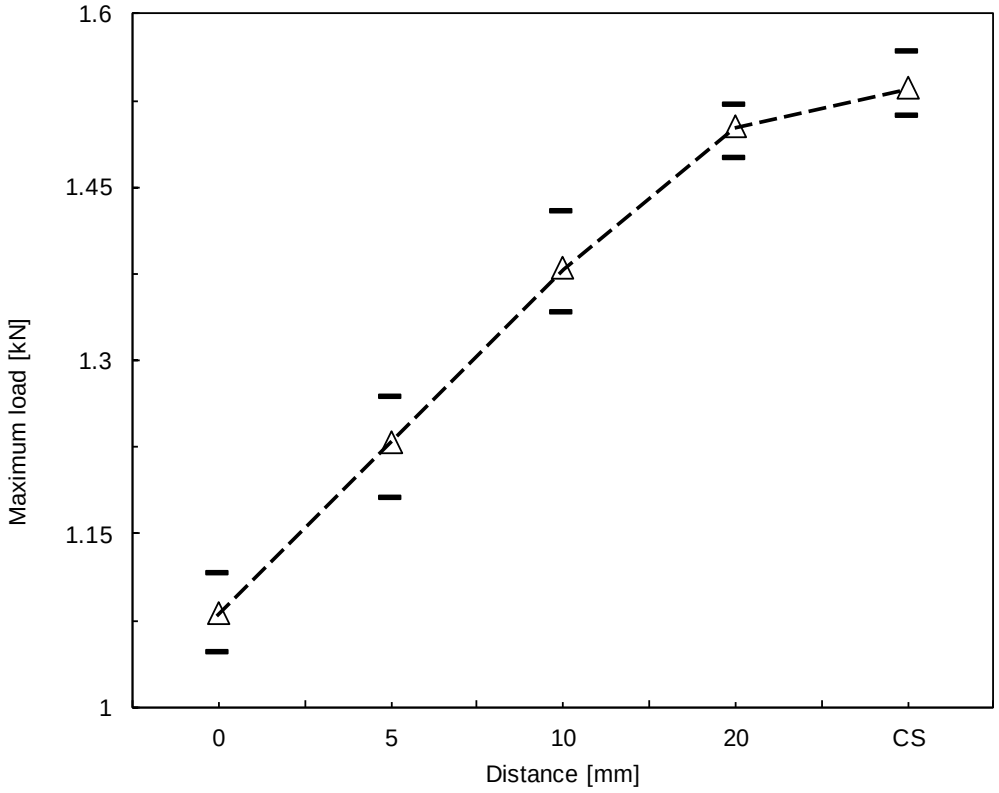

Figure 4.10- Maximum load versus distance of the hole to the indentation area for the flexural tests.

In terms of impact tests, **Figure 4.11** shows load-time and energy-time curves and the same pattern of oscillations is visible. These curves are similar to those presented in last section, and the same conclusions can be drawn about the effect of the distance of the hole.

Figure 4.12 presents the results in terms of maximum load and maximum displacement. An average maximum load of 2014 N was obtained for the control samples. This value decreases around 0.8%, 1.8%, 5.5% and 8.9% for 20, 10, 5 and 0 mm, respectively. On the other hand, the maximum displacement for the control samples is about 3.04 mm and an increase of 3.8% for 20 mm, 4.7% for 10 mm, 10% for 5 mm and 10.1% for 0 mm can be found. The IBS and elastic recuperation increase with the distance as shown in **Figure 4.13**. For the control samples, the average value of IBS is 635 N/mm and a decreasing around 2.4%, 4.2%, 12% and 19.8% can be found for 20, 10, 5 and 0 mm, respectively.

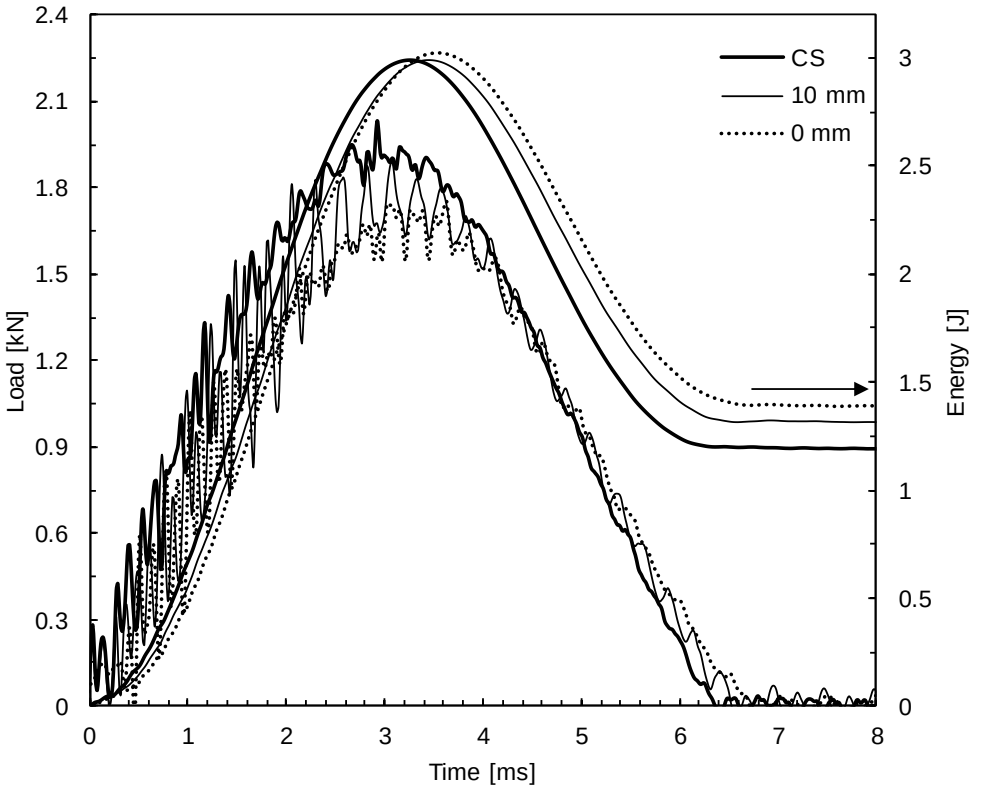

Figure 4.11- Load-time and energy-time curves for various distances of the hole for the CFRP samples subjected to impact.

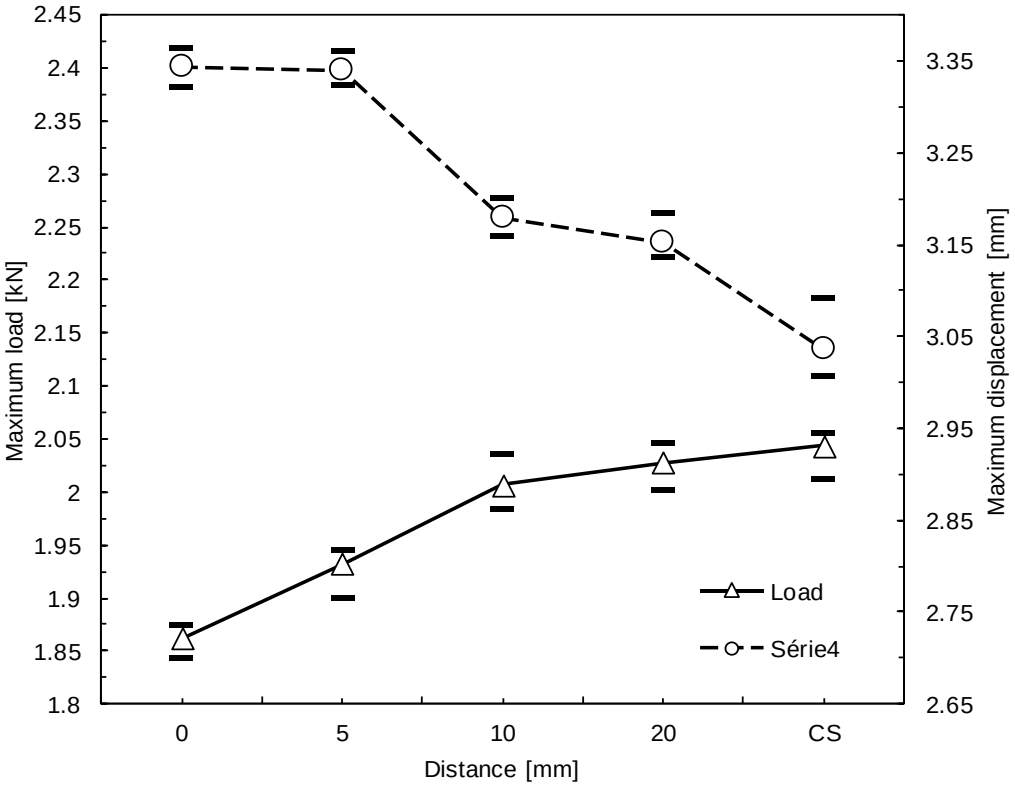

Figure 4.12- Maximum load and maximum displacement versus distance of the hole to the impact point for the impact tests.

Finally, the elastic recuperation for the CS is around 60%, and this value decreases about 1.8% for 20 mm, 4% for 10 mm, 5.1% for 5 mm and 15.5 % for 0 mm. These values reveal that, for this particular size of the hole (4 mm in diameter), distances higher than 20 mm shows a negligible effect on such parameters. In terms of damage, Figure 4.14 shows the C-Scan obtained for all configurations.

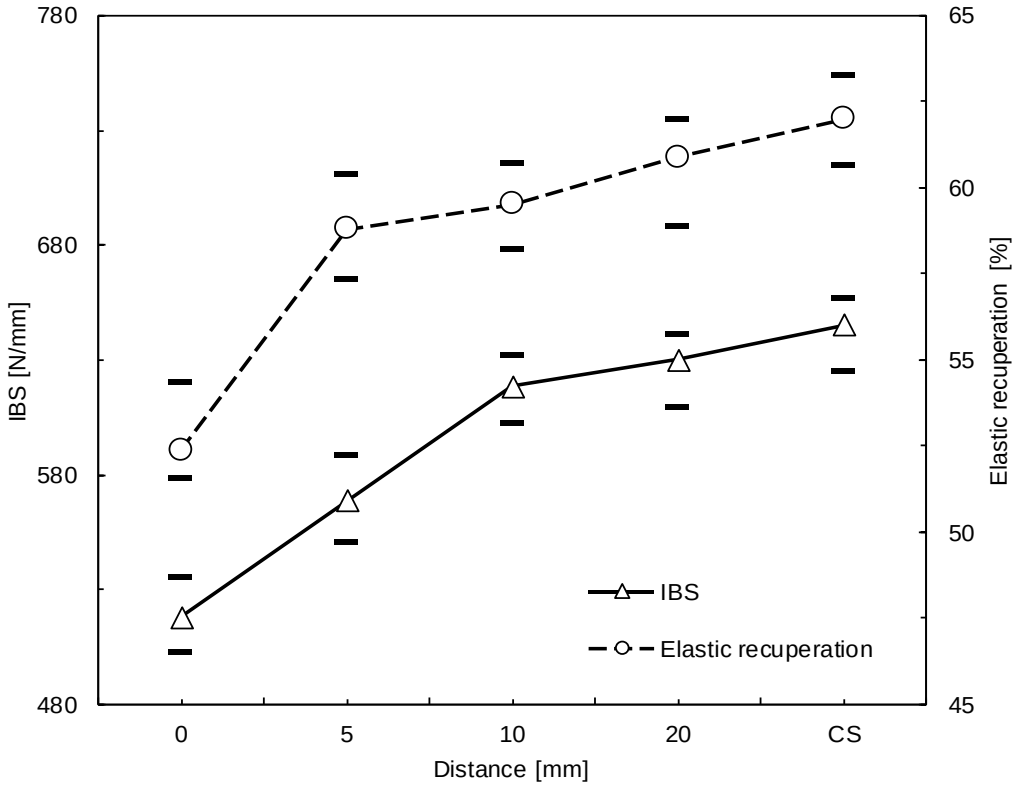

Figure 4.13- IBS and elastic recuperation versus distance of the hole to the impact point for the impact tests.

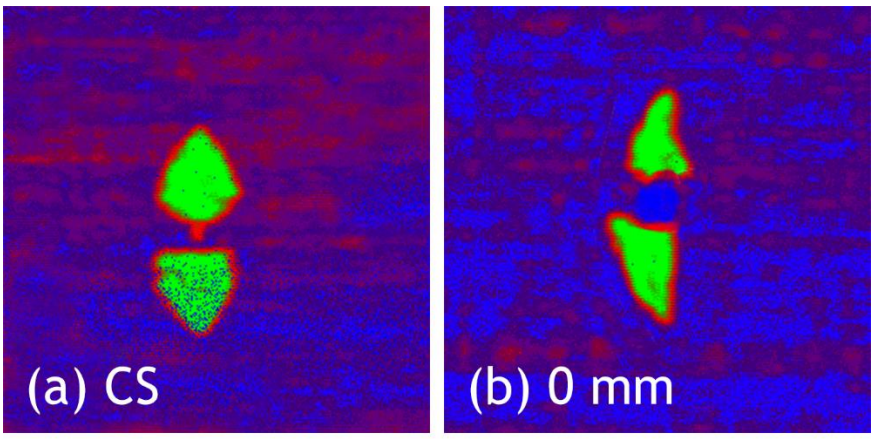

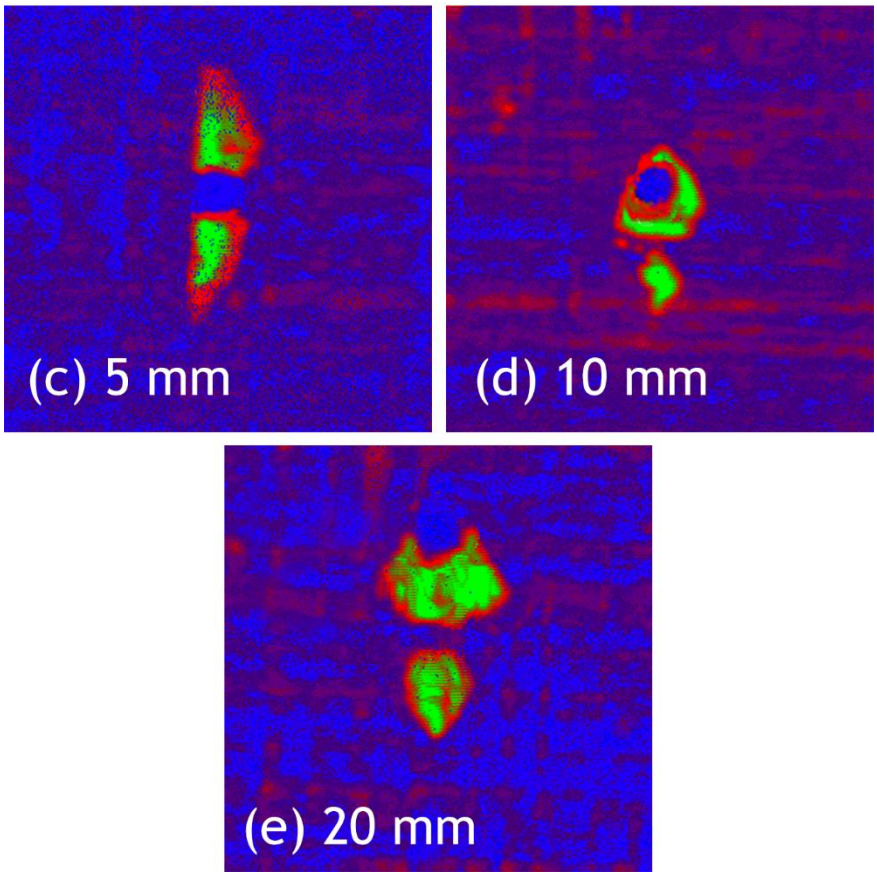

Figure 4.14- C-scan imaging of the CFRP samples.

4.3- Effect of the Distance Between the Impact point and Hole Position on Multi-Impact Strength

GFRP laminates with holes were subjected to multiple impacts in order to analyse the effect of the distance between the impact point and hole position on the fatigue performance. In this context, **Figure 4.15** shows the load-time and energy-time curves for the first impact and, one more time, these curves present oscillations as consequence of the vibrations promoted by the samples. These curves represent the typical behaviour occurred for all laminates and agree with the bibliography [3,32,36,43,68,72,79–83].

Figure 4.16 presents the results obtained in terms of maximum load and maximum displacement for the first impact. An average maximum load of 5900 N was obtained for the control samples and this value decreased around 6.1% for 20 mm, 15.4% for 10 mm, 19% for 5 mm and 22.3% for 0 mm. Contrary to what was observed for the CFRP laminates, the hole at 20 mm has a considerable effect in the case of the GFRP samples. This can be explained by the higher level of energy used (12 J). In fact, according to Reis *et al* [86], the value of P_{max} is very dependent on the impact energy. Relatively to the maximum displacement, this value is consistent with the previous results obtained for CFRP laminates.

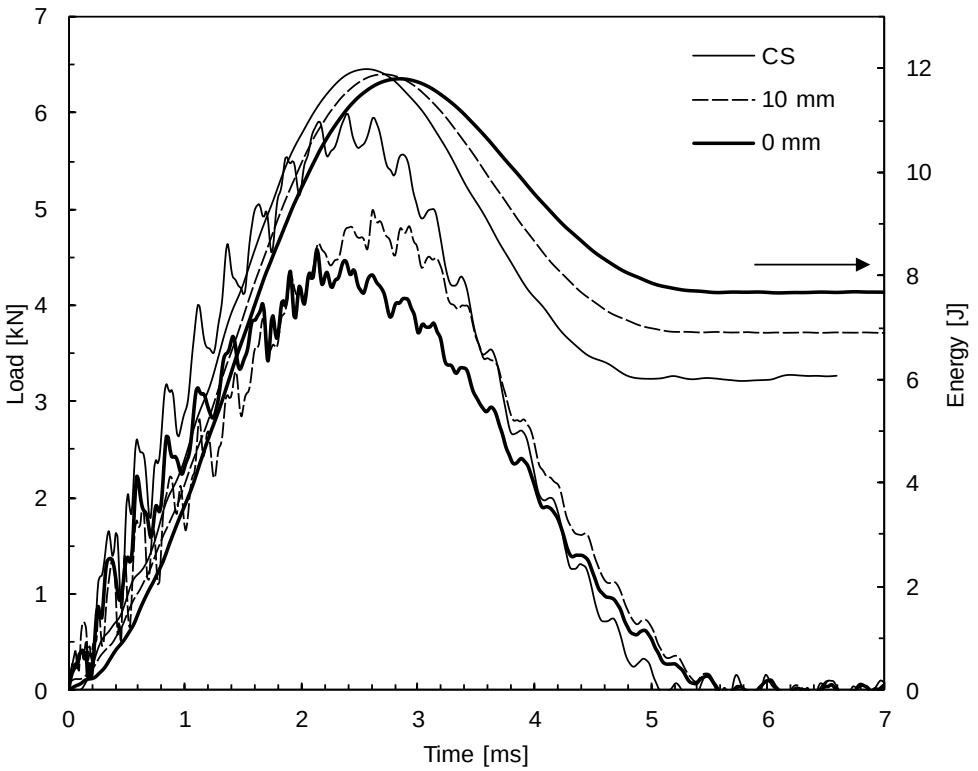

Figure 4.15- Load-time and energy-time curves for various distances of the hole for the GFRP samples subjected to impact.

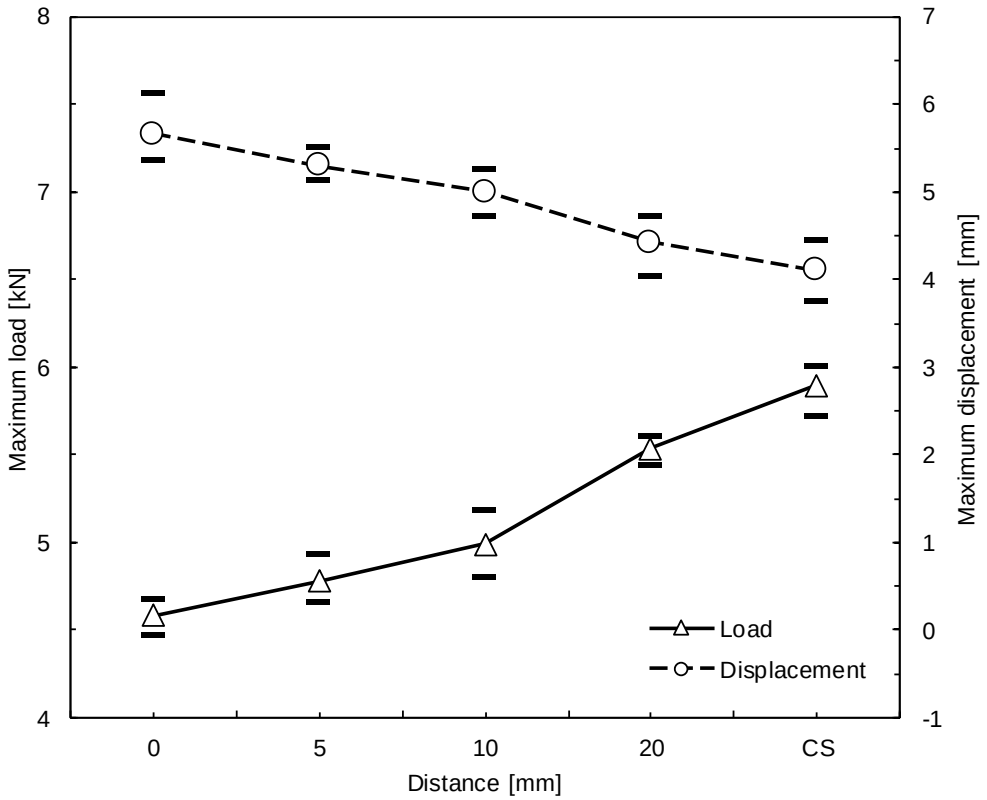

Figure 4.16- Maximum load and maximum displacement versus distance of the hole to the impact point for the GFRP samples.

For the control samples, the maximum displacement obtained was 4.1 mm, and this value is about 7.7%, 21.6%, 29% and 37.7% higher for 20 mm, 10 mm, 5 mm and 0 mm, respectively.

Figure 4.17 shows the results in terms of maximum IBS and maximum elastic recuperation. The average IBS for the CS was 1226 N/mm, and it decreased by 6.8%, 15.1%, 26.5% and 29.8%, for 20, 10, 5 and 0 mm, respectively. On the other hand, in terms of elastic recuperation, an average value of 65.7% was obtained for the control samples, while this value decreased by 10% for 20 mm, 27.6% for 10 mm, 29.7% for 5 mm and 38.5% for 0 mm. All these values are in accordance with what was obtained in section 4.2 and the same conclusions can be drawn.

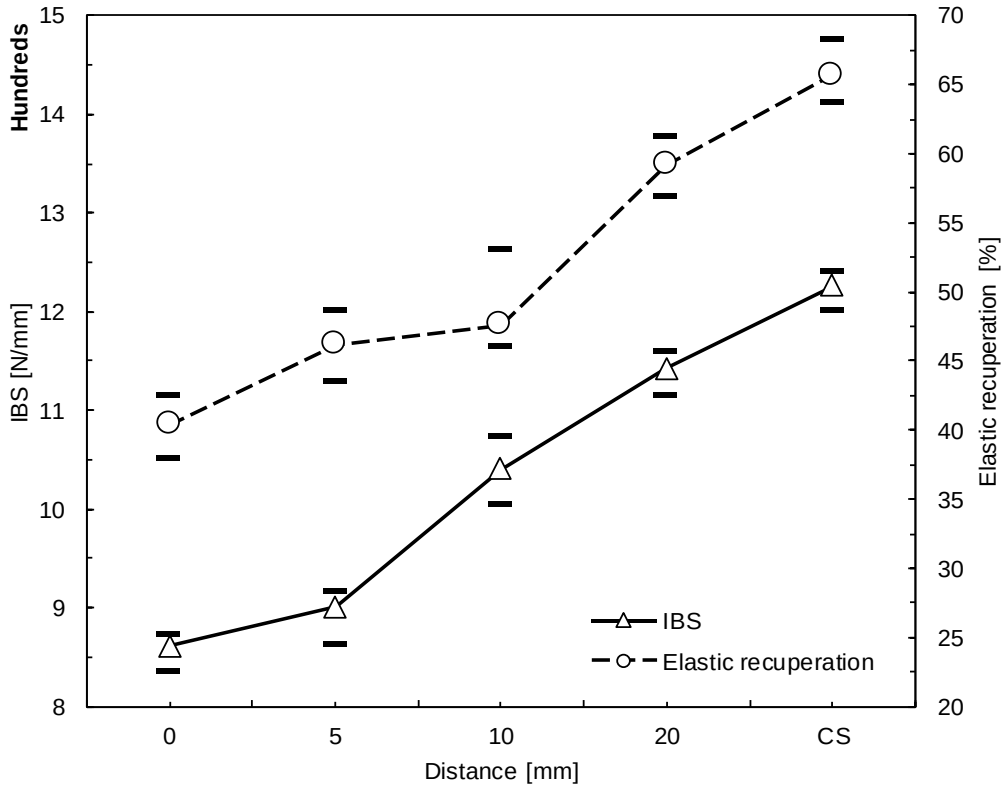

Figure 4.17- Maximum load and maximum displacement versus distance of the hole to the impact point for the GFRP samples.

Figure 4.18 presents the number of impacts to failure for the distances studied. Failure is achieved when the impactor completely moves through the samples. As expected, a clear decrease of the fatigue resistance is observed for lower distances between the hole and the impact point. Comparing the fatigue life between control samples and laminates impacted with distances of 0 mm a reduction around 68.5% can be found.

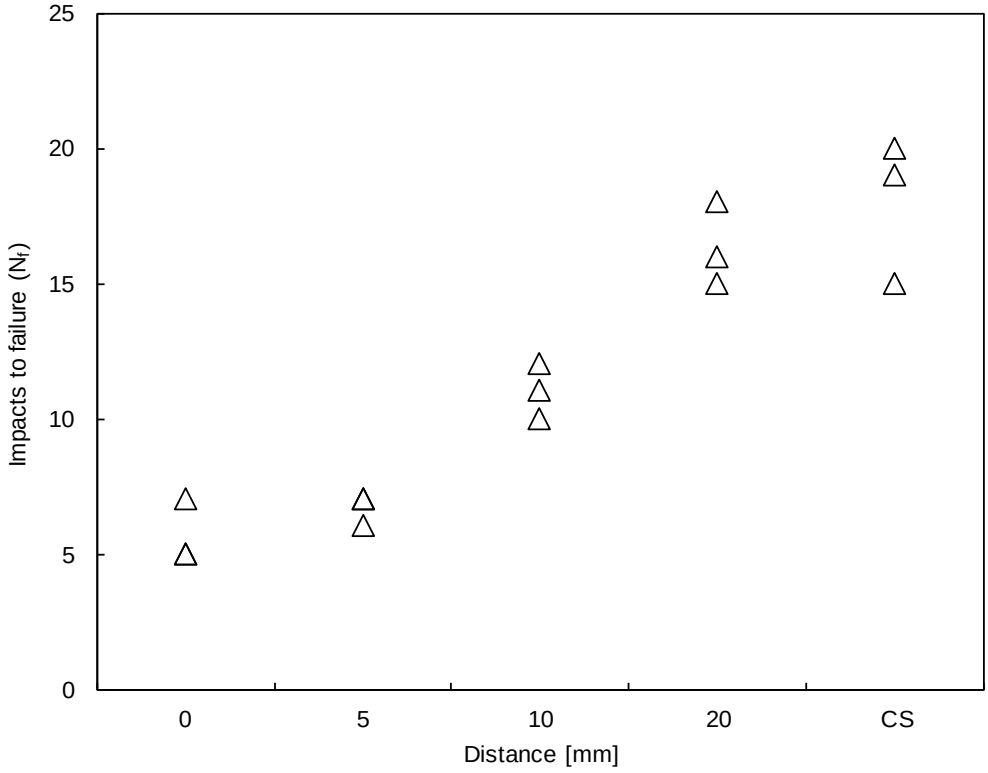

Figure 4.18- Number of impacts to failure for various distances of the hole.

Figure 4.19 shows the evolution of the load-time and energy-time curves with the impact number. As expected, the load decreases gradually until full perforation occurs. Consequently, the damage is increasing with the impacts, which is reflected in the elastic recuperation and IBS. This damage accumulation is clearly visible in **Figure 4.20** and **Figure 4.21**. **Figure 4.22** to **Figure 4.25** show the evolution of all studied variable as a function of N/N_f, which represents the impact number (N) over the number of impacts to failure (N_f).

While for the distances of 0, 5 and 10 mm the variables follow a 2nd degree polynomial trend, the CS and distance of 20 mm follow a 3rd degree polynomial trend, with a relatively high gradient in the first impacts, followed by a lower gradient region forming a small plateau, and varying again with a higher gradient after that. All variables follow an expected pattern with the number of impacts, consistent with the accumulation of damage showed through C-scan imaging and photographs.

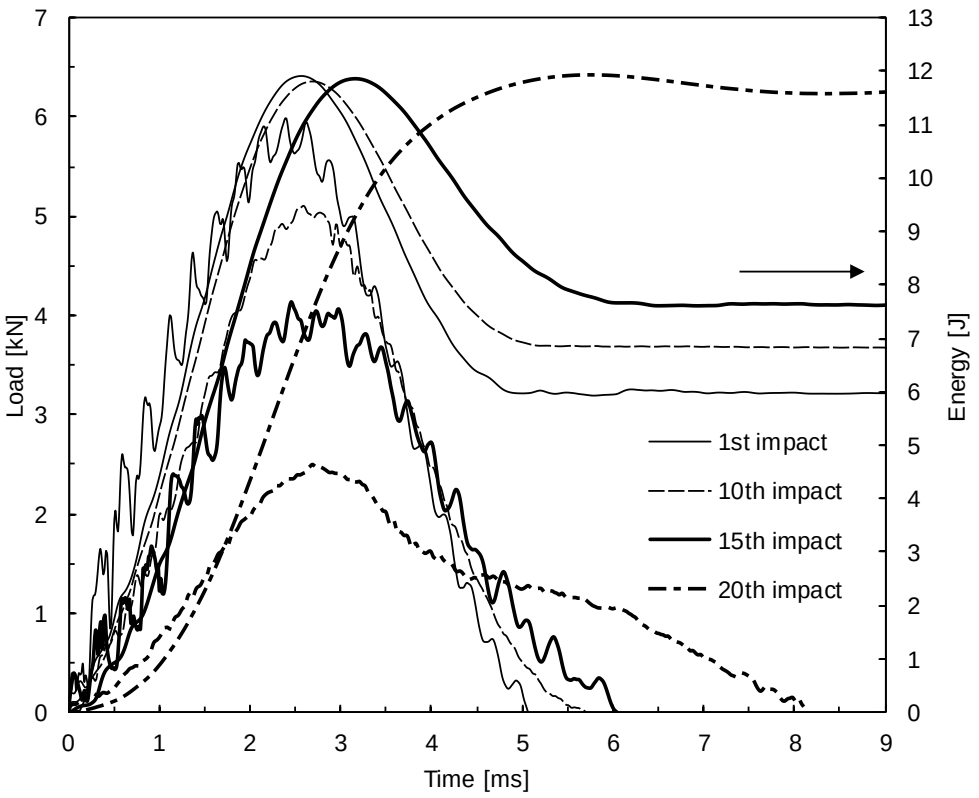

Figure 4.19- Load-time and energy-time curves for various impacts for the GFRP samples subjected to impact.

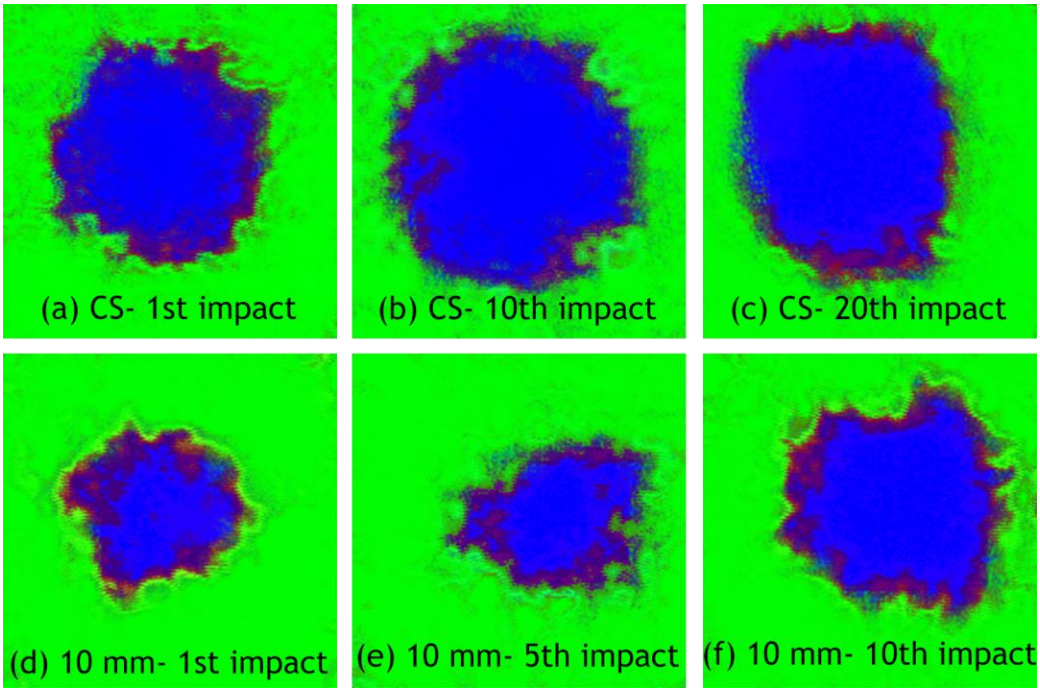

Figure 4.20- C-scan imaging of the GFRP samples.

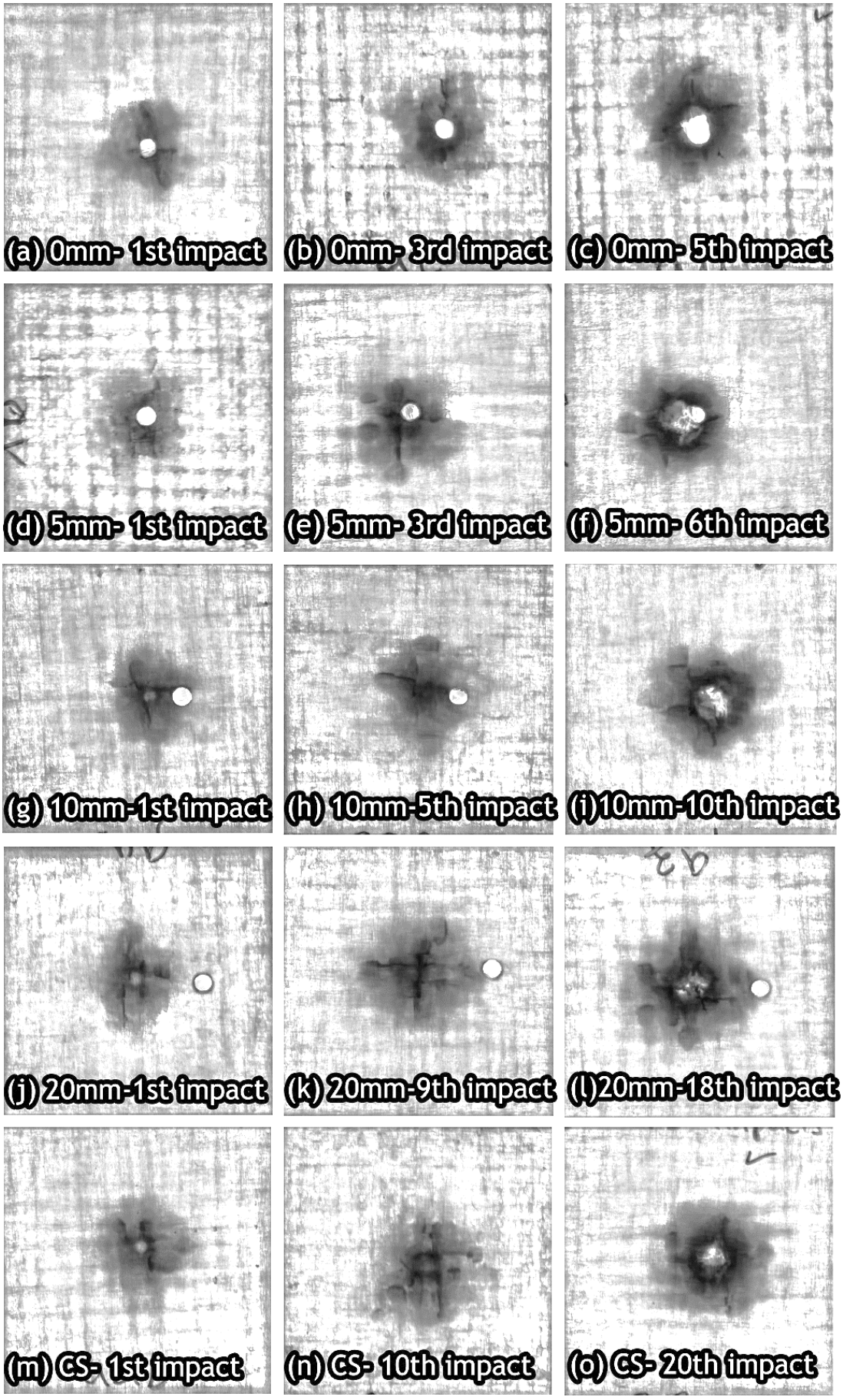

Figure 4.21- Backlit photography of the GFRP after several impacts.

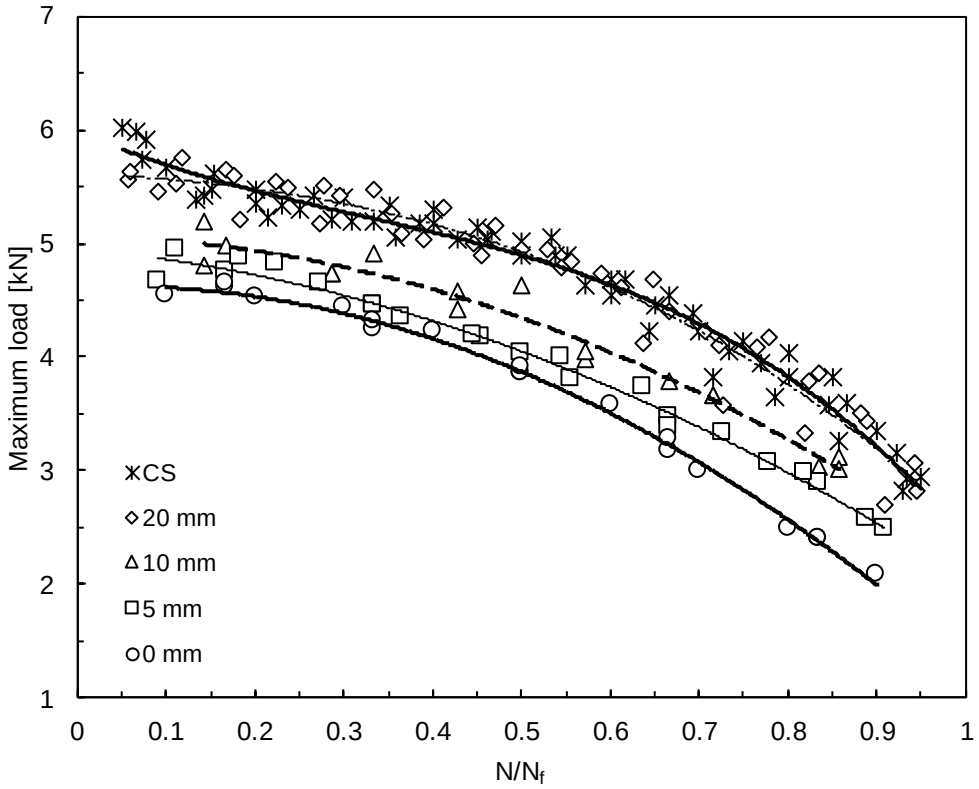

Figure 4.22- Maximum load *versus* N/N_f for the GFRP samples subjected to impact.

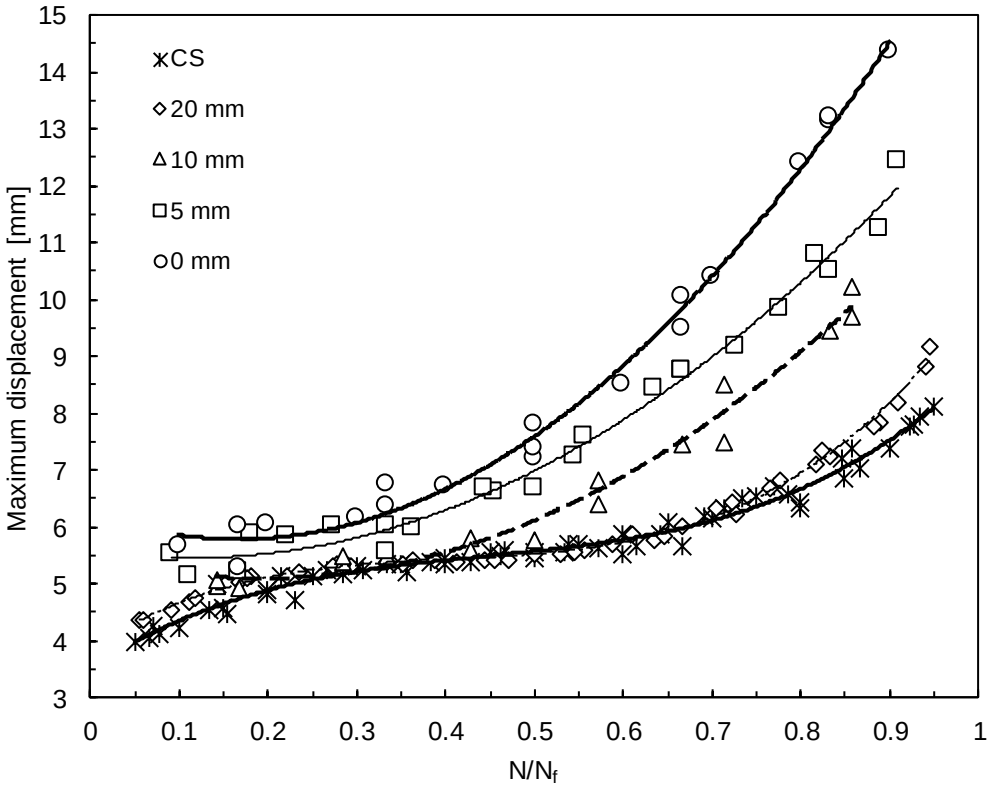

Figure 4.23- Maximum displacement *versus* N/N_f for the GFRP samples subjected to impact.

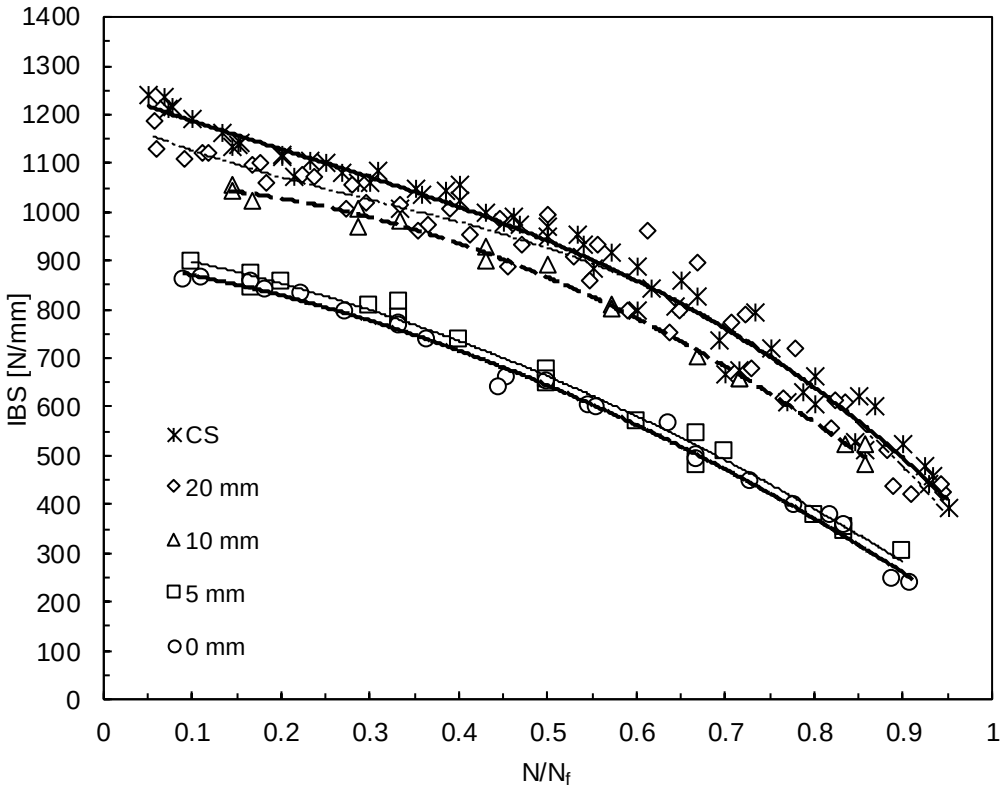

Figure 4.24- IBS *versus* N/N_f for the GFRP samples subjected to impact.

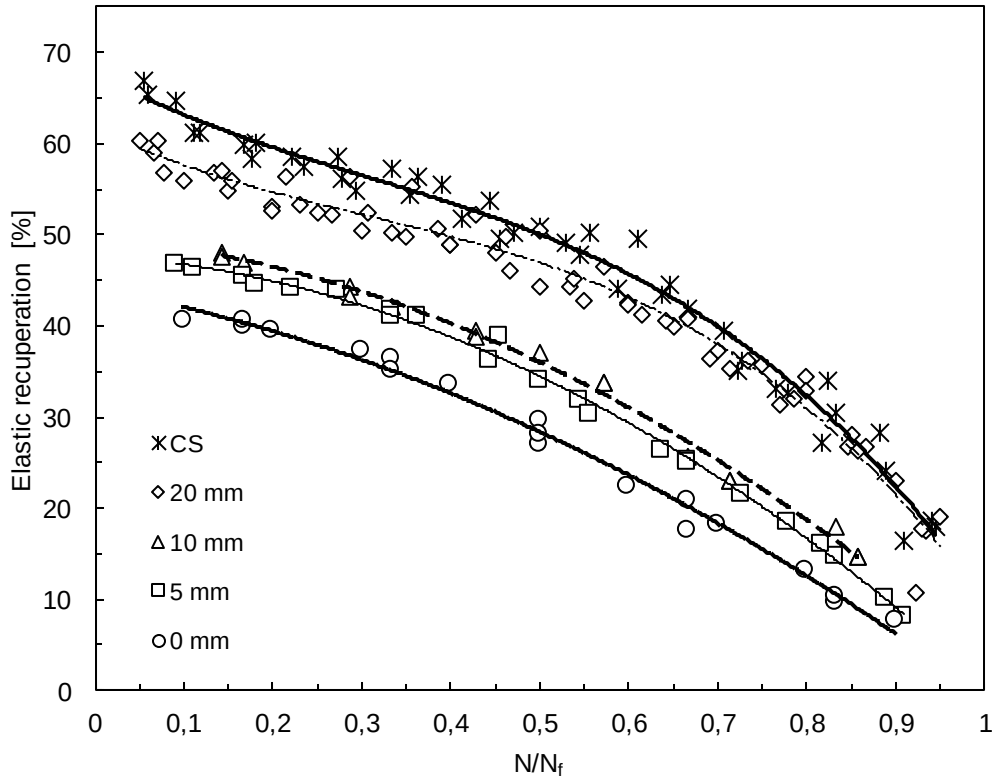

Figure 4.25- Elastic recuperation *versus* N/N_f for the GFRP samples subjected to impact.

5- Final Conclusions and Future Works

The effects of the distance between the hole and the impact point, the effects of the angle of the hole with the vertical axis and the effects of the distance of the hole to the impact point on the multi-impact resistance were analysed in detail.

From this study, it was possible to conclude that at higher impact energies the distance of 20 mm between hole and impact point promotes a decrease in maximum impact load, IBS, elastic recuperation and fatigue life, while an opposite trend occurs in terms of maximum displacement. For lower impact energies, these parameters are almost negligible. On the other hand, these effects are inversely proportional with the distance of the hole.

It was also concluded that an increasing of angles with the vertical axis promotes a decrease of the bending loads as well as the impact strength. Higher angles promote a decrease of the maximum impact load, impact bending stiffness and elastic recuperation in terms of impact strength. An opposite trend occurs in terms of maximum displacement.

It is evident from this study, that the holes have a strong effect on the impact strength. Therefore, the impact strength of composite laminates should be improved. One solution could be the use of nanoparticles, as several studies can be found in the open literature suggesting that the mechanical properties can be improved by adding, for example, nanoclay particles and carbon nanotubes. For this purpose, the effect of nanofillers on the impact strength of notched composite laminates could be studied.

On the other hand, only impacts perpendicular to the laminate surface were considered in this work. However, in the real world this might often not be the case. For example, if we consider debris hitting an aircraft while it takes off, it is easy to consider that impacts will hit at an angle with the surface of the aircraft. Therefore, it would be interesting to study the effects of the impact angle on the impact strength of composite laminates.

References

[1] M.O.W. Richardson, M.J. Wisheart, Review of low-velocity impact properties of composite materials, Compos. Part A Appl. Sci. Manuf. 27 (1996) 1123–1131.

[2] G.A. Davies, D. Hitchings, G. Zhou, Impact damage and residual strengh woven fabric glass / polyester strengths of laminates, Compos. Part A Appl. Sci. Manuf. 27 (1996) 1147–1156.

[3] R. S. R., Z. G., Impact behaviour of fibre-reinforced composite materials and structures, CRC Press Woodhead Publishing, Cambridge, 2000.

[4] D. Gay, S. V. Hoa, S.W. Tsai, Composite Materials: Design and Applications, First Edit, CRC Press, Boca Raton, 2003.

[5] S.K. Mazumdar, Composites Manufacturing: Materials, Product, and Process Engineering, First Edit, CRC Press, Boca Raton, 2001.

[6] A.B. Strong, Fundamentals of Composites manufacturing: Materials, Methods, and Applications, Second Edi, Society of Manufacturing Engineers, Dearborn, 2007.

[7] K.L. Pickering, Properties and Performance of Natural-Fibre Composites, First Edit, Woodhead Publishing, Cambridge, 2008.

[8] A.T. Nettles, M.J. Douglas, A comparison of quasi-static indentation to low-velocity impact, 2000.

[9] S. Abrate, Impact on Laminated Composites: Recent Advances, Appl. Mech. Rev. 47 (1994) 517.

[10] A.M. Amaro, P.N.B. Reis, M.F.S.F. De Moura, M.A. Neto, Influence of open holes on composites delamination induced by low velocity impact loads, Compos. Struct. 97 (2013) 239–244.

[11] J.A. Zukas, Impact Dynamics: Theory and Experiments, Maryland, 1980.

[12] I. Eriksson, C.-G. Aronsson, Strength of Tensile Loaded Graphite/Epoxy Laminates Containing Cracks, Open and Filled Holes, J. Compos. Mater. 24 (1990) 456–482.

[13] J. Backlund, C.-G. Aronsson, Tensile Fracture of Laminates with Holes, J. Compos. Mater. 20 (1986) 259–286. doi:10.1177/002199838602000304.

[14] B.G. Green, M.R. Wisnom, S.R. Hallett, An experimental investigation into the tensile strength scaling of notched composites, Compos. Part A Appl. Sci. Manuf. 38 (2007) 867–878. doi:10.1016/j.compositesa.2006.07.008.

[15] H. Suemasu, H. Takahashi, T. Ishikawa, On failure mechanisms of composite laminates

with an open hole subjected to compressive load, Compos. Sci. Technol. 66 (2006) 634–641.

[16] G.H. Erçin, P.P. Camanho, J. Xavier, G. Catalanotti, S. Mahdi, P. Linde, Size effects on the tensile and compressive failure of notched composite laminates, Compos. Struct. 96 (2013) 736–744.

[17] E. V. Iarve, D. Mollenhauer, R. Kim, Theoretical and experimental investigation of stress redistribution in open hole composite laminates due to damage accumulation, Compos. Part A Appl. Sci. Manuf. 36 (2005) 163–171.

[18] S. Dai, P.R. Cunningham, S. Marshall, C. Silva, Open hole quasi-static and fatigue characterisation of 3D woven composites, Compos. Struct. 131 (2015) 765–774.

[19] F.-K. Chang, L.B. Lessard, Damage Tolerance of Laminated Composites Containing an Open Hole and Subjected to Compressive Loadings: Part I--Analysis, J. Compos. Mater. 25 (1991) 2–43.

[20] E.J. Barbero, Introduction to Composite Materials Design, Second, CRC Press, Boca Raton, 2010.

[21] J.-M. Berthelot, Composite Materials: Mechanical Behavior and Structural Analysis (Mechanical Engineering Series), Softcover, Springer, New York, 1999.

[22] P.K. Mallick, Fibre-Reinforced Composites: Materials, Manufacturing and Design, Third Edit, CRC Press, Boca Raton, 2007.

[23] USA Department of Defense, Composite Materials Handbook - Volume 3. Polymer Matriz Composites Materials Usage, Design, and Analysis, 3 of 5 (2002).

[24] D. Hartman, M.E. Greenwood, D.M. Miller, "High strength glass fibers", Agy. (1996) 1–11.

[25] J.R. Vinson, R.L. Sierakowski, The Behavior of Structures Composed of Composite Materials, Second Edi, Kluwer Academic Publishers, Dordrecht, 2004.

[26] F.T. Wallenberger, J.C. Watson, L. Hong, Glass Fibers, ASM Hanb. 21 (2001) 27–34.

[27] H. Frenzel, U. Bunzel, R. Hassler, G. Pompe, Influence of different glass fiber sizings on selected mechanical properties of PET/glass composites, J.Adhes.Sci.Technol. 14 (2000) 651–660.

[28] ASM International. Handbook Committee., ASM handbook, Volume 21, Composites, 2001.

[29] S. Abrate, Impact on composite structures, First Edit, Cambridge University Press, New York, 1998.

[30] W.J. Cantwell, J. Morton, The impact resistance of composite materials — a review, Composites. 22 (1991) 347–362.

[31] J.M. Hodgkinson, Mechanical testing of advanced fibre composites, First Edit, CRC Press Woodhead Publishing, Boca Raton, 2000.

[32] R. Olsson, Impact response of orthotropic composite plates predicted from a one-parameter differential equation, AIAA J. 30 (1992) 1587–1596.

[33] C. Ruiz, J. Harding, Modelling impact of composite structures using small specimens, Impact Behav. Fibre-Reinforced Compos. Mater. Struct. (2000) 75–105.

[34] P.S.P. dos Santos, Resistência ao Impacto de Compósitos Híbridos, University da Beira Interior, 2010.

[35] R.L. Sierakowski, S.K. Chaturvedi, Dynamic loading and characterization of fiber-reinforced composites, 1997.

[36] P.O. Sjoblom, J.T. Hartness, T.M. Cordell, On Low-Velocity Impact Testing of Composite Materials, J. Compos. Mater. 22 (1988) 30–52.

[37] K.N. Shivakumar, W. Elber, W. Illg, Prediction of low-velocity impact damage in thin circular laminates, AIAA J. 23 (1985) 442–449.

[38] S.R. Swanson, Elastic impact stress analysis of composite plates and cylinders, in: Impact Behav. Fibre-Reinforced Compos. Mater. Struct., Elsevier, 2000: pp. 186–211.

[39] S.R. Swanson, Limits of quasi-static solutions in impact of composite structures, Compos. Eng. 2 (1992) 261–267.

[40] J.M.C. da F. Justo, Estudo do comportamento ao impacto de alta velocidade de estruturas em materiais compósitos, Faculty of Engineering of the University of Porto, 1996.

[41] W.S. Johnson, J.E. Masters, T.K. O'Brien, W.C. Jackson, C.C. Poe, The Use of Impact Force as a Scale Parameter for the Impact Response of Composite Laminates, J. Compos. Technol. Res. 15 (1993) 282.

[42] Y.K. Boey, Y.W. Kwon, Progressive damage and failure strength of notched woven fabric composites under axial loading with varying strain rates, Compos. Struct. 96 (2013) 824–832.

[43] S.M. Lee, P. Zahuta, C. Corpornrioti, Instrumented Impact and Static Indentation of Composites, J. Compos. Mater. 25 (1991) 204–222.

[44] P. a. Lagace, J.E. Williamson, P.H. Wilson Tsang, E. Wolf, S. Thomas, A Preliminary Proposition for a Test Method to Measure (Impact) Damage Resistance, J. Reinf. Plast. Compos. 12 (1993) 584–601.

[45] W. Elber, Failure Mechanics in Low-Velocity Impacts on Thin Composite Plates, Hampton, 1983.

[46] A.L. Highsmith, A Study of the Use of Contact Loading to Simulate Low Velocity Impact, 1997.

[47] L.M.S. Ferreira, Avaliação do Dano em Compósitos Laminados Devido a Impactos de Baixa Velocidade, University of Coimbra, 2006.

[48] S. Zheng, C.T. Sun, Delamination Interaction in Laminated Structures, Eng. Fract. Mech. 59 (1998) 225–240.

[49] D. Pernica, P.N.B. Reis, J.A.M. Ferreira, P. Louda, Effect of test conditions on the bending strength of a geopolymer-reinforced composite, J. Mater. Sci. 45 (2010) 744–749.

[50] C.A. Ross, R.L. Sierakowski, Studies on the impact resistance of composite plates, Composites. 4 (1973) 157–161.

[51] H. Suemasu, O. Majima, Multiple Delaminations and their Severity in Circular Axisymmetric Plates Subjected to Transverse Loading, J. Compos. Mater. 30 (1996) 441–453.

[52] B.G. Green, M.R. Wisnom, S.R. Hallett, An experimental investigation into the tensile strength scaling of notched composites, Compos. Part A Appl. Sci. Manuf. 38 (2007) 867–878.

[53] M.M. Moure, F. Otero, S.K. García-Castillo, S. Sánchez-Sáez, E.J. Barbero, Damage evolution in open-hole laminated composite plates subjected to in-plane loads, Compos. Struct. 133 (2015) 1048–1057.

[54] S.D. Pandita, K. Nishiyabu, I. Verpoest, Strain concentrations in woven fabric composites with holes, Compos. Struct. 59 (2003) 361–368.

[55] L. Toubal, M. Karama, B. Lorrain, Stress concentration in a circular hole in composite plate, Compos. Struct. 68 (2005) 31–36.

[56] V. Achard, C. Bouvet, B. Castanié, C. Chirol, Discrete ply modelling of open hole tensile tests, Compos. Struct. 113 (2014) 369–381.

[57] R. Zitoune, L. Crouzeix, F. Collombet, T. Tamine, Y.-H. Grunevald, Behaviour of composite plates with drilled and moulded hole under tensile load, Compos. Struct. 93 (2011) 2384–2391.

[58] A. Wass, C. Babcock jr., Observation of the Initiation and Progression of Damage in Compressively Loaded Composite Plates Containing a Cutout, Pasadena, 1986.

[59] C. Soutis, N.A. Fleck, Static Compression Failure of Carbon Fibre T800/924C Composite

Plate With a Single Hole, J. Compos. Mater. 24 (1990) 536–558.

[60] M. Saha, R. Prabhakaran, W.A. Waters, Compressive behavior of pultruded composite plates with circular holes, Compos. Struct. 65 (2004) 29–36.

[61] J.A.M. Ferreira, J.D.M. Costa, M.O.W. Richardson, Effect of Notch and Test Conditions on the Fatigue of a Glass-Fiber-Reinforced Polypropylene Composite, Compos. Sci. Technol. Elsevier Sci. Ltd. 57 (1997) 1243–1248.

[62] P.T. Curtis, The fatigue behaviour of fibrous composite materials, J. Strain Anal. Eng. Des. 24 (1989) 235–244.

[63] H. Hyakutake, T. Hagio, T. Yamamoto, Fatigue Failure Criterion for Notched FRP Plates, Japan Soc. Mech. Eng. 36 (1993) 2015–2019.

[64] P.N.B. Reis, J.A.M. Ferreira, F. V. Antunes, J.D.M. Costa, Fatigue Notch Sensibility of Thermoplastic Glass Fibre Composites, Mater. Sci. Forum. 514–516 (2006) 653–656.

[65] Y. Zhou, P.K. Mallick, Fatigue performance of an injection-molded short E-Glass fiber-reinforced Polyamide-6,6. II. Effects of melt temperature and hold pressure, Polym. Compos. (2011) 268–276.

[66] J.S. Huh, W. Hwang, Fatigue life prediction of circular notched CFRP laminates, Compos. Struct. 44 (1999) 163–168.

[67] C. Soutis, N.A. Fleck, P. Smith, Compression fatigue behaviour of notched carbon fibre-epoxy laminates, Int. J. Fatigue. 13 (1991) 303–312.

[68] T. Roy, D. Chakraborty, Delamination in FRP laminates with holes under transverse impact, Mater. Des. 29 (2008) 124–132.

[69] R.D. Adams, P. Cawley, A Review of defect types and non-destructive testing techniques for composites and bonded joints, Constr. Build. Mater. 3 (1989) 170–183.

[70] A.M. Amaro, P.N.B. Reis, M.F.S.F. De Moura, J.B. Santos, Damage detection on laminated composite materials using several NDT techniques, Insight Non-Destructive Test. Cond. Monit. 54 (2012) 14–20.

[71] M.F.S.F. de Moura, A.T. Marques, Prediction of low velocity impact damage in carbon-epoxy laminates, Compos. - Part A Appl. Sci. Manuf. 33 (2002) 361–368.

[72] A.M. Amaro, P.N.B. Reis, M.F.S.F. De Moura, Residual Strength after Low Velocity Impact in Carbon-Epoxy Laminates, Mater. Sci. Forum. 514–516 (2006) 624–628.

[73] A.M. Amaro, P.N.B. Reis, M.F.S.F. De Moura, Delamination effect on bending behaviour in carbon-epoxy composites, Strain. 47 (2011) 203–208.

[74] P.N.B. Reis, J.A.M. Ferreira, F. V. Antunes, M.O.W. Richardson, Effect of Interlayer

Delamination on Mechanical Behavior of Carbon/Epoxy Laminates, J. Compos. Mater. 43 (2009) 2609–2621.

[75] E.R. Green, C.J. Morrison, R.K. Luo, Simulation and Experimental Investigation of Impact Damage in Composite Plates with Holes, J. Compos. Mater. 34 (2000) 502–521.

[76] R.K. Luo, The evaluation of impact damage in a composite plate with a hole, Compos. Sci. Technol. 60 (2000) 49–58.

[77] K. Imielińska, M. Castaings, R. Wojtyra, J. Haras, E. Le Clezio, B. Hosten, Air-coupled ultrasonic C-scan technique in impact response testing of carbon fibre and hybrid: Glass, carbon and Kevlar/epoxy composites, in: J. Mater. Process. Technol., 2004: pp. 513–522.

[78] P.N.B. Reis, J.A.M. Ferreira, F. V. Antunes, J.D.M. Costa, Flexural behaviour of hybrid laminated composites, Compos. Part A Appl. Sci. Manuf. 38 (2007) 1612–1620.

[79] G.A. Schoeppner, S. Abrate, Delamination threshold loads for low velocity impact on composite laminates, Compos. Part A Appl. Sci. Manuf. 31 (2000) 903–915.

[80] N.L. Hancox, An overview of the impact behaviour of fibre-reinforced composites, Elsevier, 2000.

[81] G. Belingardi, R. Vadori, Low velocity impact tests of laminate glass-fiber-epoxy matrix composite material plates, Int. J. Impact Eng. 27 (2002) 213–229.

[82] J. Gustin, A. Joneson, M. Mahinfalah, J. Stone, Low velocity impact of combination Kevlar/carbon fiber sandwich composites, Compos. Struct. 69 (2005) 396–406.

[83] O.S. David-West, N. V. Alexander, D.H. Nash, W.M. Banks, Energy Absorption and Bending Stiffness in CFRP Laminates: The Effect of 45° Plies, Thin-Walled Struct. (2007).

[84] O.S. David-West, D.H. Nash, W.M. Banks, An experimental study of damage accumulation in balanced CFRP laminates due to repeated impact, Compos. Struct. 83 (2008) 247–258.

[85] J.M. Whitney, R.J. Nuismer, Stress Fracture Criteria for Laminated Composites Containing Stress Concentrations, J. Compos. Mater. 8 (1974) 253–265.

[86] P.N.B. Reis, J.A.M. Ferreira, Z.. . Zhang, T. Benameur, M.O.W. Richardson, Impact response of Kevlar composites with nanoclay enhanced epoxy matrix, Compos. Part B Eng. 46 (2013) 7–14.

[87] J. Wright, The English Dialect Dictionary: Being the Complete Vocabulary of All Dialect Words Still in Use, or Known to Have Been in Use During the Last Two Hundred Years, Forgotten Books, 2016.